Stability analysis of Darcy-Bénard Convection

D. Andrew S. Rees

Department of Mechanical Engineering
University of Bath
Claverton Down
Bath BA2 7AY
United Kingdom

The aim of this set of notes is two-fold. The first is to provide some teaching material in which the methods of linearised theory, weakly nonlinear theory and multiple scales theory are used for systems of engineering importance. The second is to begin the process of having a resource of detailed but mainly analytical results which may be referred to when considering convecting problems which are more complicated than those presented here.

The approach I take is quite mathematical, although it is possible to be considerably more rigorous than I have been. These notes do not comprise a comprehensive repository of information on the Darcy-Bénard problem since I concentrate only on some aspects of linearised and weakly nonlinear theories. Much more information may be gleaned from Chapter 6 of Nield and Bejan (1998) and the review chapter, Rees (1999).

Contents

1. Governing Equations and Basic Solution

1.1. Dimensional equations.

The most basic equations governing fluid flow in a porous medium are given by Darcy's law. This is a macroscopic law which relates the fluid flux to the applied pressure gradient. The constant of proportionality involves the permeability of the porous medium and the viscosity of the saturating fluid, although the dependence on viscosity was not realised by Darcy himself (Lage 1998). When considering free convection effects in a porous medium, it is common to assume the Boussinesq approximation (or, more properly, the Oberbeck-Boussinesq approximation, see Nield and Bejan 1998 p29). This yields an extra term, a buoyancy term, in Darcy's law. Therefore we take the following as the dimensional equations which govern fluid motion,

$$\overline{u} = -\frac{K}{\mu}\frac{\partial \overline{p}}{\partial \overline{x}}, \qquad \overline{v} = -\frac{K}{\mu}\frac{\partial \overline{p}}{\partial \overline{y}} + \frac{\rho_f \hat{g}\beta K}{\mu}(T - T_r), \qquad \overline{w} = -\frac{K}{\mu}\frac{\partial \overline{p}}{\partial \overline{z}}. \tag{1.1}$$

In these equations all the terms take their common meanings. The coordinate directions $\overline{x}$ and $\overline{z}$ are horizontal, while $\overline{y}$ is vertically upwards. T is the temperature of the saturated medium, T_r is a reference temperature, $\overline{p}$ is the pressure, K the permeability, μ the viscosity, $\hat{g}$ gravity, ρ_f a reference density of the fluid, and β the coefficient of cubical expansion of the fluid. The quantities $\overline{u}$, $\overline{v}$ and $\overline{w}$, correspond to the fluid flux velocities in the $\overline{x}$, $\overline{y}$ and $\overline{z}$ directions, respectively.

The full equations are completed by the equation of continuity,

$$\frac{\partial \overline{u}}{\partial \overline{x}} + \frac{\partial \overline{v}}{\partial \overline{y}} + \frac{\partial \overline{w}}{\partial \overline{z}} = 0 \tag{1.2}$$

and the energy transport equation,

$$\frac{\partial T}{\partial \overline{t}} + \overline{u}\frac{\partial T}{\partial \overline{x}} + \overline{v}\frac{\partial T}{\partial \overline{y}} + \overline{w}\frac{\partial T}{\partial \overline{z}} = \kappa\Big[\frac{\partial^2 T}{\partial \overline{x}^2} + \frac{\partial^2 T}{\partial \overline{y}^2} + \frac{\partial^2 T}{\partial \overline{z}^2}\Big], \tag{1.3}$$

where κ is the thermal diffusivity of the saturated porous medium.

1.2. Nondimensionalisation.

Equations (1.1) to (1.3) may be nondimensionalised using the transformations,

$$(\overline{x}, \overline{y}, \overline{z}) = d(x, y, z), \qquad (\overline{u}, \overline{v}, \overline{w}) = \frac{\kappa}{d}(u, v, w), \qquad \overline{p} = \frac{\kappa\mu}{K}p,$$

$$T = (T_{\max} - T_{\min})\theta + T_r, \qquad \overline{t} = \frac{d^2}{\kappa}t, \tag{1.4}$$

Here d is a representative lengthscale, which, in the present context is the depth of the layer. The nondimensional equations are

$$\frac{\partial u}{\partial x} + \frac{\partial v}{\partial y} + \frac{\partial w}{\partial z} = 0 \tag{1.5}$$

$$u = -\frac{\partial p}{\partial x}, \qquad v = -\frac{\partial p}{\partial y} + R\theta, \qquad w = -\frac{\partial p}{\partial z}. \tag{1.6}$$

$$\frac{\partial\theta}{\partial t}+u\frac{\partial\theta}{\partial x}+v\frac{\partial\theta}{\partial y}+w\frac{\partial\theta}{\partial z}=\frac{\partial^2\theta}{\partial x^2}+\frac{\partial^2\theta}{\partial y^2}+\frac{\partial^2\theta}{\partial z^2}. \tag{1.7}$$

The sole nondimensional parameter is the Darcy-Rayleigh number, R, which is defined here as

$$R=\frac{\rho_f\hat{g}\beta(T_{\max}-T_{\min})Kd}{\mu\kappa}. \tag{1.8}$$

In what follows we set $T_r=T_{\min}$.

1.3. Two-dimensional flows.

When the flow is two-dimensional, which we will take as being in the x and y directions, then we may assume that $w=0$ and all z-derivatives are zero. The equation of continuity, (1.5), is satisfied automatically when the streamfunction, ψ, is introduced according to

$$u=-\frac{\partial\psi}{\partial y},\qquad v=\frac{\partial\psi}{\partial x}. \tag{1.9}$$

In these circumstances, equations (1.6) and (1.7) reduce to

$$\frac{\partial^2\psi}{\partial x^2}+\frac{\partial^2\psi}{\partial y^2}=R\frac{\partial\theta}{\partial x} \tag{1.10}$$

$$\frac{\partial\theta}{\partial t}+\frac{\partial\psi}{\partial x}\frac{\partial\theta}{\partial y}-\frac{\partial\psi}{\partial y}\frac{\partial\theta}{\partial x}=\frac{\partial^2\theta}{\partial x^2}+\frac{\partial^2\theta}{\partial y^2}. \tag{1.11}$$

1.4. Boundary conditions.

We are considering the classical Darcy-Bénard problem, a layer of uniform thickness which is heated from below. In its most common form (i.e. impermeable and perfectly conducting boundaries) the boundary conditions are

$$y=0:\quad v=0,\ \theta=1,\ \frac{\partial p}{\partial y}=R,\qquad\qquad y=1:\quad v=0,\ \theta=0\ \frac{\partial p}{\partial y}=0. \tag{1.12}$$

When the flow is two-dimensional the boundary conditions are,

$$y=0:\quad \psi=0,\ \theta=1,\qquad\qquad y=1:\quad \psi=0,\ \theta=0. \tag{1.13}$$

1.5. Basic solution.

Given the above boundary conditions, which are uniform in the x-direction, we expect the basic solution to be independent of x. The basic state consists of no flow, a linear temperature profile and a parabolic pressure profile:

$$u=v=w=\psi=0,\qquad \theta=1-y,\qquad p=R(y-\tfrac{1}{2}y^2)+\text{constant}. \tag{1.14}$$

2. Linearised Stability Theory

2.1. The classical Darcy-Bénard problem..

In the last section we determined the basic flow, which is given by (1.14), and we will now perform a linear stability analysis to determine conditions under which the solution can be expected to exist in practice. This is undertaken by perturbing the basic solution and finding the growth rate of the perturbation, which is assumed to be small in magnitude. Therefore we set

$$\psi = \Psi, \qquad \theta = 1 - y + \Theta, \tag{2.1}$$

into equations (1.10) and (1.11). If we assume that $|\Psi| \ll 1$ and $|\Theta| \ll 1$, and neglect products of the perturbations, we obtain

$$\Psi_{xx} + \Psi_{yy} = R\Theta_x, \qquad \Theta_t - \Psi_x = \Theta_{xx} + \Theta_{yy}, \tag{2.2}$$

where subscripts denote partial derivatives. This partial differential system may be transformed into ordinary differential eigenvalue form by means of the substitutions,

$$\Psi = f(y)e^{\lambda t}\cos kx, \qquad \Theta = g(y)e^{\lambda t}\sin kx, \tag{2.3}$$

where λ is the **exponential growth rate**, and k is the **wavenumber** of the disturbance. Equations (2.2) reduce to

$$f'' - k^2 f = Rkg, \qquad g'' - k^2 g = kf + \lambda g, \tag{2.4a,b}$$

subject to the homogeneous boundary conditions

$$f = g = 0 \quad \text{on} \quad y = 0, 1. \tag{2.4c}$$

These equations form an eigenvalue problem for λ in terms of k and R. The solution may be obtained analytically in terms of sines:

$$f = -\frac{k^2 + \pi^2 + \lambda}{k} A \sin \pi y, \qquad g = A \sin \pi y, \tag{2.5a,b}$$

with

$$\lambda = \frac{Rk^2}{k^2 + \pi^2} - (k^2 + \pi^2), \tag{2.5c}$$

Here the overall amplitudes of f and g are unspecified, i.e. A may take any value. The variation of λ with R and k is given by (2.5c), and negative values correspond to disturbances which decay exponentially with time and which are therefore stable. Positive values imply that the disturbance is unstable, and it grows exponentially although, clearly, there will come a point when nonlinear effects take over and moderate the evolution of the instability. However, when $\lambda = 0$ we have what is known as **marginal stability** or **neutral stability** since the disturbance neither grows nor decays. Setting $\lambda = 0$ in (2.5c) yields what is called the **neutral stability curve**,

$$R = \frac{(k^2 + \pi^2)^2}{k^2}, \tag{2.6}$$

which is plotted in Figure 2.1. We note that points which lie above the curve correspond to instability, while the points below correspond to stable disturbances. Thus the minimum point

of the curve is of great importance, for below it disturbances of all wavenumbers decay with time, while above it there is a range of wavenumbers, k, for which disturbances grow. This minimum point corresponds to the **critical values**:

$$R_c = 4\pi^2, \qquad k_c = \pi. \tag{2.7}$$

This particular wavenumber corresponds to convection cells which have an aspect ratio of exactly unity.

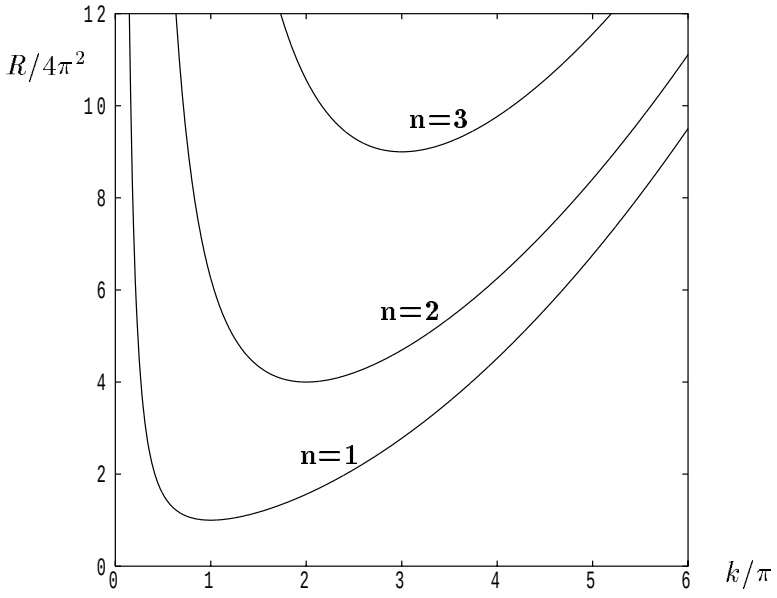

Figure 2.1. Showing the neutral curves for the first three modes for the classical Darcy-Bénard problem. These are denoted by $n = 1$, 2 and 3.

The solutions given by (2.5) and (2.6) are not the only ones which are admissible. We also have

$$f = -\frac{k^2 + n^2\pi^2 + \lambda}{k} A \sin n\pi y, \qquad g = A \sin n\pi y, \tag{2.8a,b}$$

with

$$\lambda = \frac{Rk^2}{k^2 + n^2\pi^2} - (k^2 + n^2\pi^2), \tag{2.8c}$$

and hence $\lambda = 0$ yields

$$R = \frac{(k^2 + n^2\pi^2)^2}{k^2}, \tag{2.9}$$

the minimum value of which is

$$R_c = 4n^2\pi^2, \qquad \text{at} \qquad k_c = n\pi. \tag{2.10}$$

Here n must be an integer in order that the upper boundary conditions are satisfied. Thus (2.8a,b) corresponds to n convective rolls stacked above one another. But both (2.9) and (2.10) show that the critical value of R is well above those given by (2.5) and (2.6), and which are also

shown in Figure 2.1. These modes are known as higher modes, and while they exist theoretically, it is rare that they become important practically.

We note that solutions of the form (2.3) also exist in finite cavities where the sidewalls are impermeable ($\Psi = 0$) and insulated ($\Theta_x = 0$). In such cases only certain wavenumbers are permissible in order to fit a whole number of identical convecting cells into the cavity.

2.2. The effect of form-drag.

This the first of various extensions to the Darcy-Benard problem which we will consider briefly. Here we will consider the effect on stability of the presence of form-drag. The extra term which arises in Darcy's law is quadratic and reflects the increased resistance to flow at relatively high microscopic fluid velocities within the porous medium. The governing equations are given by

$$u_x + v_y + w_z = 0, \tag{2.11}$$

$$u(1+Gq) = -p_x, \qquad v(1+Gq) = -p_y + R\theta, \qquad w(1+Gq) = -p_z, \tag{2.12}$$

$$\theta_t + u\theta_x + v\theta_y + w\theta_z = \theta_{xx} + \theta_{yy} + \theta_{zz}, \tag{2.13}$$

where the fluid flux speed, q, is given by

$$q^2 = u^2 + v^2 + w^2, \tag{2.14}$$

and the inertia parameter G is defined as

$$G = \frac{\tilde{K}\rho\kappa}{\mu d}, \tag{2.15}$$

where $\tilde{K}$ is a material parameter.

On introduction of the streamfunction for two-dimensional flows, the above equations reduce to

$$(1+Gq)(\psi_{xx} + \psi_{yy}) + G(\psi_x q_x + \psi_y q_y) = R\theta_x, \tag{2.16}$$

$$\theta_t + \psi_x\theta_y - \psi_y\theta_x = \theta_{xx} + \theta_{yy}. \tag{2.17}$$

In terms of the streamfunction we have

$$q^2 = \psi_x^2 + \psi_y^2. \tag{2.18}$$

The basic flow and temperature fields are given by equation (1.14). If we introduce the small-amplitude perturbations, (2.1), then the linearised stability equations are

$$\Psi_{xx} + \Psi_{yy} = R\Theta_x, \qquad \Theta_t - \Psi_x = \Theta_{xx} + \Theta_{yy}, \tag{2.19}$$

which are identical to those given in (2.2) for the classical Darcy-Bénard problem. Therefore we conclude that form-drag does not affect the criterion for the onset of convection in a porous medium. However, appearances can be deceptive, for inertia does affect strongly the resulting flow at higher Rayleigh numbers and the range of influence of instability mechanisms, but such aspects are dealt with in Rees (1996) and Strange and Rees (1996).

2.3. The effect of the Brinkman terms.

When a porous medium has high porosity Darcy's law no longer remains valid near bounding surfaces where the sparsity of the solid phase means that the no-slip condition, which is prevalent in standard fluid mechanics, must be applied near such surfaces. Brinkman (1947) undertook an analysis of the effective viscosity of a swarm of particles in a fluid and this has been used as a means of extending Darcy's law for rigid porous media to account for the transition between a porous medium and a clear fluid as the porosity tends towards unity.

For two-dimensional flows the governing nondimensional equations are

$$-D\nabla^4\psi + \nabla^2\psi = R\theta_x, \tag{2.20a}$$

$$\theta_t + \psi_x\theta_y - \psi_y\theta_x = \nabla^2\theta, \tag{2.20b}$$

and the boundary conditions are

$$y = 0: \quad \psi = \psi_y = 0, \quad \theta = 1, \qquad y = 1: \quad \psi = \psi_y = \theta = 0. \tag{2.21}$$

Here D is the Darcy number given by

$$D = \frac{\mu_{\text{eff}} K}{\mu_f d^2} \tag{2.22}$$

where μ_{eff} is the effective viscosity.

The basic velocity and temperature fields are unchanged from those given in (1.14), and therefore the linearised perturbation equations are

$$-D\nabla^4\Psi + \nabla^2\Psi = R\Theta_x, \qquad \Theta_t - \Psi_x = \nabla^2\Theta. \tag{2.23}$$

On substitution of

$$\Psi = f(y)e^{\lambda t}\cos kx, \qquad \Theta = g(y)e^{\lambda t}\sin kx \tag{2.24}$$

into (2.23) we obtain the equations,

$$-D(f'''' - 2k^2f'' + k^4f) + f'' - k^2f = Rkg, \qquad g'' - k^2g = kf + \lambda g. \tag{2.25}$$

These equation cannot be solved analytically and therefore numerical methods must be employed. This system was first solved by Walker and Homsy (1977) who found that the critical value of R not only depends on the value of D, but increases as D increases, as shown in Figure 2.2. This figure shows R_c as a function of D where the values of R have been minimised with respect to the wavenumber k. The minimising wavenumbers are shown in Figure 2.3. For small values of D, R_c is very close to $4\pi^2$, which confirms that the small-D limit recovers the well-known Darcy-flow criterion. At the opposite extreme, for large values of D, the curve becomes a straight line satisfying the asymptotic relation,

$$R/D \sim 1708 \tag{2.26}$$

The large-D limit corresponds to the clear fluid limit, and it should therefore be no surprise that the parameter, R/D, is the Rayleigh number of a clear fluid (on taking $\mu_{\text{eff}} = \mu_f$), and that the numerical value in (2.26) is precisely the onset criterion for the classical Bénard problem with

no-slip boundary conditions. A quick glance at Figure 2.3 shows how the critical wavenumber varies from π when D is very small, to 3.116, the Bénard value, when D is large.

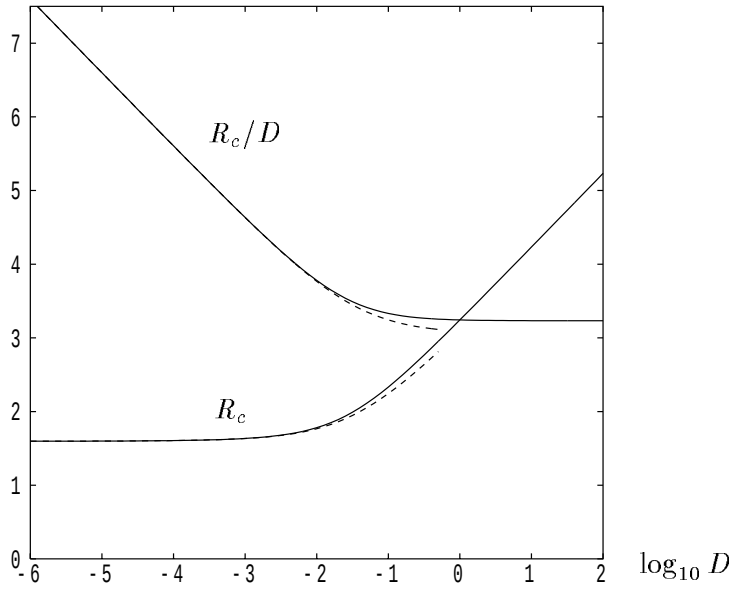

Figure 2.2. Neutral curves for the onset of convection for $10^{-6} \leq D \leq 10^2$. Values are presented in terms of the Darcy-Rayleigh number, R_c, and the clear-fluid Rayleigh number R_c/D. The dashed line denotes the small-D asymptotic values given in (2.27a).

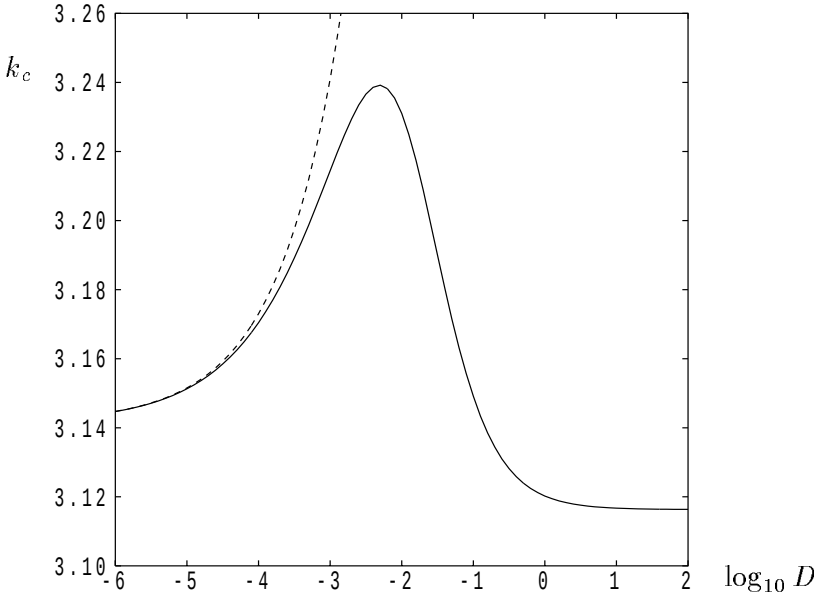

Figure 2.3. Critical wavenumber, k_c, for the onset of convection for $10^{-6} \leq D \leq 10^2$. The dashed curve denotes the small-D asymptotic values given in (2.27b).

Space does not permit an asymptotic analysis of the small-D limit, which may be undertaken analytically — for further details see Rees (2001). But this limit is not straightforward to analyse since the small parameter, D, multiplies the term with the highest derivative. Therefore the mathematical problem requires a singular perturbation analysis using the method of matched asymptotic expansions. Briefly, the flow is split into three regions, two of thickness $O(D^{1/2})$ near the upper and lower surfaces, and a main core region where Darcy flow prevails. Rees (2001) has shown that the critical Rayleigh number and wavenumber take the following form for small values of D:

$$R_c = 4\pi^2[1 + D^{1/2} + (2\pi^2 + 3 + \pi\sqrt{3}\tanh(\sqrt{3}\pi/2)D + \cdots], \tag{2.27a}$$

$$k_c = \pi[1 + D^{1/2} + \cdots]. \tag{2.27b}$$

2.4. The effect of a horizontal pressure gradient.

In the above sections the neutral stability criterion may also be obtained by setting $\lambda = 0$ in the disturbance equations, (2.4) and (2.25), and by then solving the resulting equations as an eigenvalue problem for R in terms of k. The analysis given for the classical Darcy flow case in §2.1 demonstrates that this procedure is correct for the problems studied thus far. Stability problems where this is so satisfy what is called the **exchange of stabilities**. However most stability problems do not satisfy exchange of stabilities, and the most common flows where this is so are boundary layer flows. Such problems are characterised by having an overall mean flow which is perpendicular to the axes of the convective cells, and therefore instability, when it occurs, consists of convective rolls which move in the same direction as the mean flow. This is also true for channel flows such as plane Poiseuille flow. Therefore in this subsection and the following two we will consider the effect of a horizontal pressure gradient on the above stability criteria.

Let us return to the classical Darcy-Bénard problem but add in a nondimensional horizontal pressure gradient of magnitude H. From equation (1.6) this means that we have a basic horizontal flow given by

$$u = H, \qquad \Rightarrow \qquad \psi = -H(y - \tfrac{1}{2}), \tag{2.28}$$

where we have chosen the constant of integration for ψ to be such that ψ is antisymmetric about $y = \frac{1}{2}$. The equations for the small-amplitude perturbations are now

$$\Psi_{xx} + \Psi_{yy} = R\Theta_x, \qquad \Theta_t - \Psi_x + H\Theta_x = \Theta_{xx} + \Theta_{yy}. \tag{2.29}$$

The perturbation analysis given in §2.2 does not carry through easily in the form given there, and therefore we will assume that the small-amplitude perturbations are given by

$$\Psi = \text{Real}\Big[f(y)e^{\lambda t}e^{ikx}\Big], \qquad \Theta = \text{Real}\Big[-ig(y)e^{\lambda t}e^{ikx}\Big]. \tag{2.30}$$

Comparison of (2.29) with (2.3) shows that they are precisely the same if f and g are real. The resulting equations for f and g are

$$f'' - k^2 f = Rkg, \qquad g'' - k^2 g = kf + (\lambda + iHk)g, \tag{2.31}$$

and the solution of this eigenvalue problem is precisely the same as for the $H = 0$ case given in §2.2 except that

$$\text{Imag}[\lambda] = -Hk. \tag{2.32}$$

If this is substituted back into, say, the expression for Ψ given in (2.30) and the real part is taken (noting that $f(y)$ remains real), then we have

$$\Psi = \text{Real}\Big[f(y)e^{ik(x-Ht)}\Big] = f(y)\cos k(x - Ht), \tag{2.33}$$

at onset. This solution shows that the convecting pattern not only moves in the direction of the mean basic flow but it also travels at exactly the same speed. This result was first shown by Prats (1967). It may also be shown, by transformation into a frame of reference which is moving at the same velocity as the basic flow, that even the nonlinear equations of motion become independent of H, which implies that the ensuing nonlinear motions are independent of H.

2.5. The combined effect of form drag and a horizontal pressure gradient.

We now combine two of the above cases, namely form-drag and a horizontal pressure gradient. We have already shown that neither of them affect the critical Rayleigh number and wavenumber when they operate separately, although the latter causes the convection cells to move horizontally. The aim here is to determine whether these two effects interact and alter the stability criterion.

The two-dimensional equations of motion are as given in (2.16) and (2.17), but are repeated for completeness' sake:

$$(1 + Gq)(\psi_{xx} + \psi_{yy}) + G(\psi_x q_x + \psi_y q_y) = R\theta_x, \tag{2.34a}$$

$$\theta_t + \psi_x\theta_y - \psi_y\theta_x = \theta_{xx} + \theta_{yy}, \tag{2.34b}$$

and the boundary conditions are that

$$y = 0: \quad \psi = \tfrac{1}{2}Q, \quad \theta = 1, \qquad y = 1: \quad \psi = -\tfrac{1}{2}Q, \quad \theta = 0. \tag{2.35}$$

Here we have introduced the value Q which is related to the size of the pressure gradient, $-H$, by the relation,

$$H = Q(1 + G|Q|). \tag{2.36}$$

By this we mean that the horizontal pressure gradient causes the horizontal fluid motion $u = Q$, and therefore the basic flow and temperature fields are

$$\psi = -Q(y - \tfrac{1}{2}), \qquad \Theta = 1 - y. \tag{2.37}$$

After perturbing about this basic state, the equations for the disturbances are

$$\Big[1 + G|Q|\Big]\nabla^2\Psi + G|Q|\Psi_{yy} = R\Theta_x, \tag{2.38}$$

$$\Theta_t - \Psi_x + Q\Theta_x = \nabla^2\Theta, \tag{2.39}$$

and these are to solved subject to the usual homogeneous boundary conditions.

On introducing

$$\Psi = \text{Real}\Big[f(y)e^{\lambda t}e^{ikx}\Big], \qquad \Theta = \text{Real}\Big[-ig(y)e^{\lambda t}e^{ikx}\Big]. \tag{2.40}$$

we eventually find that

$$R = \frac{(\pi^2 + k^2)^2}{k^2} + G|Q|\frac{(\pi^2 + k^2)(2\pi^2 + k^2)}{k^2}. \tag{2.41}$$

Clearly this result implies that the critical Rayleigh number increases when the product $G|Q|$ increases from zero. We also get $\mathrm{Imag}(\lambda) = -kQ$, which implies that the cells travel with the same velocity as the induced mean flow.

We may minimise this value of R with respect to k to obtain

$$R_c = \pi^2\Big[(1+G|Q|)^{1/2} + (1+2G|Q)^{1/2}\Big]^2. \tag{2.42}$$

and

$$k_c = \pi\Big[\frac{1+2G|Q|}{1+G|Q|}\Big]^{1/4}. \tag{2.43}$$

We can see easily that the critical wavenumber also increases with $G|Q|$.

It is straightforward to use (2.42) and (2.43) to determine how R_c and k_c vary in both the small and large $G|Q|$ limits. When $G|Q|$ is very small, then

$$R_c \sim (4 + 6G|Q| + \cdots)\pi^2, \qquad k_c \sim (1 + \tfrac{1}{4}G|Q| + \cdots)\pi, \tag{2.44}$$

and, when $G|Q|$ is very large, then

$$R_c \sim [3 + 2\sqrt{2}]G|Q|\pi^2, \qquad k_c \sim 2^{1/4}\pi. \tag{2.45}$$

Although it has not been proved above, the present case is the first one considered in these notes where the orientation of the convection roll is important in determining the onset criterion. If we denote perturbation quantities by upper-case characters, then the perturbation equations for the fully three dimensional equations of motion are given by

$$U_x + V_y + W_z = 0, \tag{2.46}$$

$$U(1+2G|Q|) = -P_x, \tag{2.47}$$

$$V(1+G|Q|) = -P_y + R\Theta, \tag{2.48}$$

$$W(1+G|Q|) = -P_z, \tag{2.49}$$

$$\Theta_t + Q\Theta_x - V = \Theta_{xx} + \Theta_{yy} + \Theta_{zz}. \tag{2.50}$$

These equations admit solutions of the form,

$$\begin{pmatrix} U \\ V \\ W \\ \Theta \\ P \end{pmatrix} = \exp\Big[\lambda t + ik[(x-Qt)\cos\phi - z\sin\phi]\Big] \begin{pmatrix} U^* \cos\pi y \\ V^* \sin\pi y \\ W^* \cos\pi y \\ \Theta^* \sin\pi y \\ P^* \cos\pi y \end{pmatrix}, \tag{2.51}$$

where the starred quantities are constants, and where ϕ is the orientation of the roll away from having its axis in the z-direction.

For arbitrary wavenumbers and roll orientations neutral stability occurs when

$$R = (\pi^2 + k^2)(1+G|Q|) + \frac{\pi^2 + k^2}{k^2\Big[\dfrac{\cos^2\phi}{1+2G|Q|} + \dfrac{\sin^2\phi}{1+G|Q|}\Big]}. \tag{2.52}$$

For general roll orientations the minimising value of the wavenumber is

$$k_c = \pi\Big[\frac{1+G|Q|}{1+2G|Q|}\cos^2\phi + \sin^2\phi\Big]^{-1/4}, \tag{2.53}$$

while the corresponding critical Rayleigh number is

$$R_c = \pi^2(1+G|Q|)\Big[1+\Big(\frac{1+2G|Q|}{1+G|Q|(1+\sin^2\phi)}\Big)^{1/2}\Big]^2. \tag{2.54}$$

We are now in a position to determine which orientation of the roll gives the earliest onset of convection. A brief examination of (2.54) is sufficient to be convinced that $\phi = \frac{1}{2}\pi$ is the preferred orientation, i.e. the rolls have axes in the direction of the mean flow. Thus we get

$$R_c = 4\pi^2(1+G|Q|), \qquad k_c = \pi, \tag{2.55}$$

when $\alpha = \frac{1}{2}\pi$.

This analysis also appears as Rees (1997).

2.6. The combined effect of the Brinkman terms and a horizontal pressure gradient.

We will concentrate solely on the two-dimensional case, even though it is highly likely that three-dimensional flows with axes in the direction of the mean flow will form the most unstable roll direction. The following work is original and does not yet appear in the research literature.

Once more the basic temperature profile is linear, but the velocity profile is no longer constant. We find that ψ is given by

$$\psi = -\tfrac{1}{2}Q\Big[\frac{(y-\frac{1}{2})\cosh\alpha - D^{1/2}\sinh(2\alpha(y-\frac{1}{2}))}{\frac{1}{2}\cosh\alpha - D^{1/2}\sinh\alpha}\Big], \tag{2.56}$$

where $\alpha = 1/(2D^{1/2})$, and therefore

$$\psi_y = -\tfrac{1}{2}Q\Big[\frac{\cosh\alpha - \cosh 2\alpha(y-\frac{1}{2})}{\frac{1}{2}\cosh\alpha - D^{1/2}\sinh\alpha}\Big] \equiv -F(y), \tag{2.57}$$

which defines the velocity function $F(y)$. When D is small (i.e. α is large) the second terms in both the numerator and denominator of the fraction in (2.57) are negligible compared with their respective first terms when y is not close to either 0 or 1. Therefore the flow in the main bulk of the layer is $-\psi_y \sim Q$.

The linearised perturbation equations are now

$$-D\nabla^4\Psi + \nabla^2\Psi = R\Theta_x, \qquad \Theta_t - \Psi_x + F(y)\Theta_x = \nabla^2\Theta. \tag{2.58}$$

On substitution of

$$\Psi = \mathrm{Real}\Big[f(y)e^{\lambda t}e^{ikx}\Big], \qquad \Theta = \mathrm{Real}\Big[-ig(y)e^{\lambda t}e^{ikx}\Big]. \tag{2.59}$$

into (2.58) we obtain the equations,

$$-D(f'''' - 2k^2f'' + k^4f) + f'' - k^2f = Rkg, \qquad g'' - k^2g = kf + (\lambda - kFi)g. \tag{2.60a,b}$$

This system, being complex, is more difficult to solve than is (2.25). Further, we cannot reduce it to the case given by (2.25) where the horizontal flow is absent because the coefficient of g on the right hand side of (2.60b) is a function of y. In the Table below we see how the wavespeed depends on D when $Q = 1$. Although the wavespeed is greater than Q, it is always less than the maximum speed in the layer. It also tends towards Q as $D \to 0$.

D	R	Imag$[\lambda]/k$	$F_{\max}$	Imag$[\lambda]/F_{\max}$
0.005	51.367	1.139	1.163	0.9798
0.010	60.452	1.183	1.233	0.9592
0.020	77.951	1.226	1.312	0.9343
0.030	95.208	1.248	1.355	0.9207
0.040	112.387	1.261	1.383	0.9124
0.050	129.530	1.270	1.401	0.9067

Table 2.1. Comparison of the neutral Rayleigh numbers, wavespeeds and maximum channel velocities of various values of D for $k = \pi$ and $Q = 1$.

2.7. Concluding remarks.

The above analyses do not exhaust the possibilities for linearised theory. We have not touched upon thermal dispersion, local thermal nonequilibrium between the solid and fluid phases, non-Newtonian effects, inclination, throughflow effects, solutal effects, rotation, anisotropy, variable permeability, nonBoussinesq effects, layering etc.. We have also assumed that the domain in which the convection is taking place is unbounded, whereas in practice it will be confined. All of these different modifications to the classical case will affect the onset criterion. The methods presented above may be used in the great majority of these cases and combinations of the cases to determine onset criteria.

However useful onset criteria are, it is nevertheless essential to consider nonlinear effects. For the classical Darcy-Bénard problem we assumed a disturbance in the form of a single roll, but there is no *a priori* reason that a single roll will appear in practice, even though this is true, at least for moderate Rayleigh numbers, for the classical problem. The nonlinear behaviour of convection can and does show quite a variety of behaviours depending on the precise modification to the classical case. For example convection may take the form of square or rectangular cells (which may be thought of as the superposition of two different rolls), hexagonal cells (three rolls), or concentric circles (an integral over all possible roll directions). Further, although linear theory gives a criterion for the onset of convection, this is not always reflected in practice as flows may sometimes appear at Rayleigh numbers which are below the onset criterion.

It is at this point that weakly nonlinear theory can be used to examine the stability characteristics at Rayleigh numbers which are fairly close to the critical value. Within this regime important information such as pattern selection, wavenumber selection, modes of secondary instability and postcritical rates of heat transfer may be decided. It is frequently the case that such qualitative information remains correct well into the strongly nonlinear regime.

3. 2D weakly nonlinear solutions

3.1. Weakly nonlinear scalings.

Consider weak convection where the amplitude of the roll disturbance is of $O(\epsilon)$ where ϵ is considered to be asymptotically small in this section. The roll will have a wavenumber which is precisely equal to $k_c = \pi$ and the Rayleigh number will be an $O(\epsilon^2)$ amount above its critical value of $4\pi^2$. We will work with the perturbation to the basic conduction state, $\psi = 0, \theta = 1 - y$, given by (2.1):

$$\psi = \Psi, \qquad \theta = 1 - y + \Theta, \tag{3.1}$$

and therefore Ψ and Θ satisfy the fully nonlinear equations,

$$\Psi_{xx} + \Psi_{yy} = R\Theta_x, \qquad \Theta_t - \Psi_x + \Psi_x\Theta_y - \Psi_y\Theta_x = \Theta_{xx} + \Theta_{yy}, \tag{3.2}$$

subject to $\Psi = \Theta = 0$ at both $y = 0$ and $y = 1$. We will introduce the following asymptotic series for Ψ and Θ:

$$\begin{pmatrix} \Psi \\ \Theta \end{pmatrix} = \epsilon \begin{pmatrix} \Psi_1 \\ \Theta_1 \end{pmatrix} + \epsilon^2 \begin{pmatrix} \Psi_2 \\ \Theta_2 \end{pmatrix} + \epsilon^3 \begin{pmatrix} \Psi_3 \\ \Theta_3 \end{pmatrix} + \cdots \tag{3.3}$$

and, to reflect the fact that the Rayleigh number is an $O(\epsilon^2)$ amount above its critical value, we set

$$R = R_0 + \epsilon^2 R_2 + \cdots \qquad \text{where} \quad R_0 = R_c = 4\pi^2. \tag{3.4}$$

Finally, since the exponential growth of linearised disturbances is proportional to the difference of the Rayleigh number from the critical value we will rescale time according to

$$\tau = \tfrac{1}{2}\epsilon^2 t, \tag{3.5}$$

where the numerical factor has been determined *a posteriori* in order to get convenient coefficients later. On substitution of (3.4) and (3.5) into equation (3.2) we obtain

$$\Psi_{xx} + \Psi_{yy} = (R_0 + \epsilon^2 R_2)\Theta_x, \tag{3.6a}$$

$$\tfrac{1}{2}\epsilon^2\Theta_\tau - \Psi_x + \Psi_x\Theta_y - \Psi_y\Theta_x = \Theta_{xx} + \Theta_{yy}. \tag{3.6b}$$

3.2. Leading order roll solution.

On substitution of (3.3) into (3.6) we obtain a sequence of linear equations at each subsequent order in ϵ. At $O(\epsilon)$ we obtain the homogeneous system,

$$\nabla^2\psi_1 - R_0\theta_{1x} = 0, \qquad \nabla^2\theta_1 + \psi_{1x} = 0, \tag{3.7}$$

which is identical to the linearised equations (2.2) with the exception of the absence of the time derivative term. Therefore we may take the following as its solution,

$$\psi_1 = \frac{2}{\pi} A \sin\pi x \sin\pi y, \qquad \theta_1 = \frac{1}{\pi^2} A \cos\pi x \sin\pi y. \tag{3.8}$$

This is the $k = \pi$ version of the linearised solutions of §2.1. Once more we have chosen the numerical coefficients on the right hand sides to yield the most convenient coefficients later.

In (3.8) the unknown amplitude, A, is assumed to be a function of τ in order to reflect the fact that convection becomes stronger in time when R is above R_c.

3.3. $O(\epsilon^2)$ equations and solutions.

At $O(\epsilon^2)$ the equations for ψ_2 and θ_2 are

$$\nabla^2\psi_2 = R_0\theta_2, \tag{3.9a}$$

$$\begin{aligned}\nabla^2\theta_2 - \psi_{2x} &= \psi_{1x}\theta_{1y} - \psi_{1y}\theta_{1x} \\ &= \frac{1}{\pi}A^2\sin 2\pi y\end{aligned} \tag{3.9b}$$

The solution of this system is

$$\psi_2 = 0, \qquad \theta_2 = -\frac{1}{4\pi^3}A^2\sin 2\pi y. \tag{3.10}$$

Thus there is no flow at this order, but the fact that θ_2 is not dependent on x means that it is from this term that the mean rate of surface heat transfer may be obtained. Thus

$$\theta_y\Big|_{y=0} \sim \frac{\partial}{\partial y}\Big[1 - y - \frac{1}{4\pi^3}\epsilon^2 A^2\sin 2\pi y\Big]_{y=0} = -1 - \frac{A^2\epsilon^2}{2\pi^2}. \tag{3.11}$$

It remains now to determine an expression for A^2.

3.4. $O(\epsilon^3)$ equations, solvability conditions and amplitude equations.

At $O(\epsilon^3)$ the equations are

$$\begin{aligned}\nabla^2\psi_3 - R_0\theta_{3x} &= R_2\theta_{1x}, \\ &= -\frac{1}{\pi}R_2 A\sin\pi x\sin\pi y,\end{aligned} \tag{3.12a}$$

$$\begin{aligned}\nabla^2\theta_3 - \psi_{3x} &= \psi_{1x}\theta_{2y} - \psi_{1y}\theta_{2x} + \psi_{2x}\theta_{1y} - \psi_{2y}\theta_{1x} \\ &= \frac{1}{2\pi^2}A^3\cos\pi x(\sin\pi y - \sin 3\pi y) + \frac{1}{2\pi^2}A_\tau\cos\pi x\sin\pi y.\end{aligned} \tag{3.12b}$$

If we now attempt to solve these equations then we are left with an enormous amount of algebraic difficulty because all but one of the inhomogeneous terms are proportional to the eigensolutions of the left hand side differential operators (as given by the solutions (3.8)). The result of such an endeavour would show us that a solution can only be obtained when R_2 and A satisfy the appropriate equation. However, it is possible to find the equation for R_2 and A without solving the system (3.12), but simply by insisting that the system has a solution.

We proceed by rewriting (3.12a) and (3.12b) in the form,

$$\nabla^2\psi_3 - R_0\theta_{3x} = \mathcal{R}_1, \qquad \nabla^2\theta_3 - \psi_{3x} = \mathcal{R}_2, \tag{3.13a,b}$$

for convenience, and by forming the integral,

$$I = \int_0^2\int_0^1 \Big[(\nabla^2\psi_3 - R_0\theta_3)\psi_1 + (\nabla^2\theta_3 - \psi_{3x})R_0\theta_1\Big]\,dy\,dx. \tag{3.14}$$

On integration by parts, and by taking into account the fact that $\psi_n = \theta_n = 0$ on $y = 0$ and $y = 1$ for all values of n, we find that

$$I = \int_0^2 \int_0^1 \left[(\nabla^2 \psi_1 - R_0 \theta_1) \psi_3 + (\nabla^2 \theta_1 - \psi_{1x}) R_0 \theta_3 \right] dy\, dx = 0. \tag{3.15}$$

That this integral is zero follows from the fact that the terms in the small square brackets are zero by definition; see equations (3.7). On substitution of (3.13) into (3.14) this implies that

$$I = \int_0^2 \int_0^1 \left[\mathcal{R}_1 \psi_1 + \mathcal{R}_2 \theta_1 R_0 \right] dy\, dx = 0. \tag{3.16}$$

The application of the condition by substitution of the definitions of $\mathcal{R}_1$ and $\mathcal{R}_2$ yields the following equation for the amplitude, A, in terms of R_2,

$$A_\tau = R_2 A - A^3. \tag{3.17}$$

Such equations are known as **amplitude equations**, or as a **Landau equations**. The condition (3.16) is an example of a **solvability condition**, or an **orthogonality condition**.

3.5. Solutions of the amplitude equation and stability.

It is straightforward to see that equation (3.17) has the following steady solutions,

$$A = 0 \quad \text{for all values of } R_2, \qquad A = \pm R_2^{1/2} \quad \text{when } R_2 > 0. \tag{3.18a}$$

It is also possible to obtain the unsteady solution,

$$A = \pm \frac{R_2^{1/2}}{\sqrt{1 - C e^{-2R_2 \tau}}}, \tag{3.18b}$$

where C is an arbitrary constant. In fact, if we apply the initial condition, $A = A_0 > 0$ at $\tau = 0$, then the unsteady solution is

$$A = \frac{R_2^{1/2}}{\sqrt{1 - \left(1 - \dfrac{R_2}{A_0}\right) e^{-2R_2 \tau}}}. \tag{3.19}$$

This latter solution shows that A grows towards $R_2^{1/2}$ when $0 < A_0 < R_2^{1/2}$, and that A decreases towards $R_2^{1/2}$ when $A_0 > R_2^{1/2}$. Thus we expect the $A = 0$ solution to be unstable when $R_2 > 0$.

Let us consider the stability of the $A = 0$ solution. If we assume that $|A|$ is very small in equation (3.17) then the equation may be approximated by

$$A_\tau = R_2 A, \tag{3.20}$$

whose solutions are $A \propto e^{R_2 \tau}$. Therefore this disturbance grows when $R_2 > 0$ and decays when $R_2 < 0$; this result is consistent with the linearised analysis since R_2 represents the deviation of R away from the critical value. Thus, for a very small amplitude initial disturbance the flow grows in strength exponentially at first, but eventually this growth is attenuated by nonlinear effects as given in (3.19).

The above steady solutions and their stability characteristics may be summarised in the following figure which is an example of a **bifurcation diagram**. Here the dashed line indicates that the solution is unstable, while the continuous lines indicate stability. The shape of the system of curves is reminiscent of the pitchfork used by farmers to gather in the hay, and therefore this bifurcation is known as a **pitchfork bifurcation**. Moreover, since the outer two branches are stable, it is also known more precisely as a **supercritical pitchfork bifurcation**.

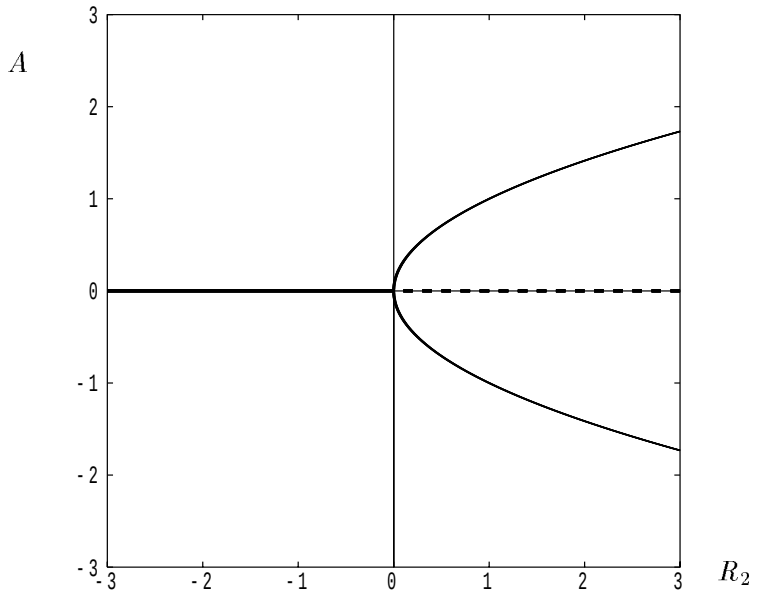

Figure 3.1. Showing the bifurcation diagram for the supercritical bifurcation given by the steady solutions of (3.17). The solid lines denote stable solutions, while the dashed lines correspond to unstable solutions.

4. 2D weakly nonlinear theory: Eckhaus instability

4.1. Horizontal scalings for wavenumber changes.

In the last section we considered the weakly nonlinear evolution of a single roll of wavenumber $k_c = \pi$ at Rayleigh numbers which are $O(\epsilon^2)$ above the critical value $4\pi^2$. The aim of this section is to relax the assumption that the wavenumber is precisely equal to π, and to allow k to vary by a small amount. To determine the admissable size of variation we may set $k = \pi + \delta$, where $|\delta| \ll 1$, in the expression for R given in (2.6); hence

$$R = \frac{(k^2+\pi^2)^2}{k^2} = 4\pi^2 + 4\delta^2 + \cdots. \tag{4.1}$$

Given that $R - R_c$ was taken to be $O(\epsilon^2)$ in the last section, this means that δ and ϵ may be taken to be of the same magnitude. Therefore we will allow k to vary from π by $O(\epsilon)$ amounts.

If we allow such a variation in k then we need to deal with quantities such as $\cos(\pi + \epsilon K)x$ or $\exp[i(\pi + \epsilon K)x]$, and this may be done using the method of multiple scales. Therefore we allow solutions to vary on two lengthscales, one of which is of $O(1)$ and the other of $O(1/\epsilon)$. The former takes account of the main convection pattern whereas the latter allows for "slow" changes over many wavelengths. Thus we define the slow x-scale, X, according to

$$X = \epsilon x, \tag{4.2}$$

and therefore we replace

$$\frac{\partial}{\partial x} \qquad \text{by} \qquad \frac{\partial}{\partial x} + \epsilon\frac{\partial}{\partial X} \tag{4.3}$$

in equations (3.6). Therefore equations (3.6) become

$$\Psi_{xx} + 2\epsilon\Psi_{xX} + \epsilon^2\Psi_{XX} + \Psi_{yy} = (R_0 + \epsilon^2 R_2)(\Theta_x + \epsilon\Theta_X), \tag{4.4a}$$

$$\tfrac{1}{2}\epsilon^2\Theta_\tau - \Psi_x - \epsilon\Psi_X + (\Psi_x\Theta_y - \Psi_y\Theta_x) + \epsilon(\Psi_X\Theta_y - \Psi_y\Theta_X) = \Theta_{xx} + 2\epsilon\Theta_{xX} + \epsilon^2\Theta_{XX} + \Theta_{yy}. \tag{4.4b}$$

4.2. $O(\epsilon)$ solutions.

We substitute the expansion (3.3) into equations (4.4) to obtain a sequence of equations at each order in ϵ. At leading order we recover equations (3.7) but we will not take (3.8) as our solution as this representation is real. Rather, it is more convenient to use a complex representation of the same solution:

$$\psi_1 = -\frac{i}{\pi}\left[Ae^{i\pi x} - \bar{A}e^{-i\pi x}\right]\sin\pi y, \tag{4.5a}$$

$$\theta_1 = \frac{1}{2\pi^2}\left[Ae^{i\pi x} + \bar{A}e^{-i\pi x}\right]\sin\pi y. \tag{4.5b}$$

Here we will allow A to vary with both X and τ. The small changes in wavenumber will be equivalent to setting A to be proportional to $\exp(iKX)$.

4.3. $O(\epsilon^2)$ solutions.

At $O(\epsilon^2)$ the equations are

$$\begin{aligned}\nabla^2\psi_2 - R_0\theta_{2x} &= R_0\theta_{1X} - 2\psi_{1xX}\\ &= 0,\end{aligned} \tag{4.6a}$$

$$\begin{aligned}\nabla^2\theta_2 + \psi_{2x} &= \psi_{1x}\theta_{1y} - \psi_{1y}\theta_{1x} - \psi_{1X} - 2\theta_{1xX}\\ &= \frac{1}{\pi}A\bar{A}\sin 2\pi y.\end{aligned} \tag{4.6b}$$

So, although there are officially extra terms on the right hand sides of these equations, as compared with (3.9), they cancel, and therefore the $O(\epsilon^2)$ is as given in (3.10).

4.4. $\underline{O(\epsilon^3)\text{ solutions}}$.

The equations at this order are

$$\begin{aligned}\nabla^2\psi_3 - R_0\theta_{3x} &= R_1\theta_{2X} + R_2\theta_{1X} - 2\psi_{2xX} - \psi_{1XX}\\ &= \frac{iR_2}{2\pi}\Big[Ae^{i\pi x} - \bar{A}e^{-i\pi x}\Big]\sin\pi y + \frac{i}{\pi}\Big[Ae^{i\pi x} - \bar{A}e^{-i\pi x}\Big]\sin\pi y\\ &\quad + \text{nonresonant terms},\end{aligned} \tag{4.7a}$$

$$\begin{aligned}\nabla^2\theta_3 + \psi_{3x} &= \psi_{2x}\theta_{1y} - \psi_{2y}\theta_{1x} + \psi_{1x}\theta_{2y} - \psi_{1y}\theta_{2x}\\ &\quad + \psi_{1X}\theta_{1y} - \psi_{1y}\theta_{1X} - \psi_{2X} - 2\theta_{2xX} - \theta_{1XX}\\ &= \frac{1}{4\pi^2}\Big[A_\tau e^{i\pi x} + \bar{A}_\tau e^{-i\pi x}\Big] - \frac{1}{2\pi^2}A\bar{A}\Big[Ae^{i\pi x} + \bar{A}e^{-i\pi x}\Big]\sin\pi y\,\cos 2\pi y\\ &\quad - \frac{1}{2\pi^2}\Big[A_{XX}e^{i\pi x} + \bar{A}_{XX}e^{-i\pi x}\Big]\sin\pi y + \text{nonresonant terms}.\end{aligned} \tag{4.7b}$$

For this complex system the solvability condition changes very slightly. Using the notation, $\mathcal{R}_1$ and $\mathcal{R}_2$, to denote the right hand sides of equations (4.7a) and (4.7b), respectively, then the solvability condition may be written in the form,

$$\int_0^2\int_0^1\Big[\mathcal{R}_1\hat{\psi}_1 + R_0\mathcal{R}_2\hat{\theta}_1\Big]\,dy\,dx = 0. \tag{4.8}$$

Here the terms $\hat{\psi}_1$ and $\hat{\theta}_1$ are given by the $\bar{A}$ coefficients of the $O(\epsilon)$ eigensolutions:

$$\hat{\psi}_1 = \frac{i}{\pi}e^{-i\pi x}\sin\pi y, \qquad \hat{\theta}_1 = \frac{1}{2\pi^2}e^{-i\pi x}\sin\pi y. \tag{4.9}$$

Application of this condition yields the amplitude equation,

$$A_\tau = R_2A + 4A_{XX} - A^2\bar{A}. \tag{4.10}$$

We may take as the steady solution of (4.10) what is called the **phase winding** solution,

$$A = \sqrt{R_2 - 4K^2}e^{iKX}, \tag{4.11}$$

The physical effect of the complex exponential here is to vary the phase of the convecting roll relative to that given by $e^{i\pi x}$. If we substitute (4.11) into (4.5b) we obtain

$$\theta_1 = \frac{\sqrt{R_2 - 4K^2}}{2\pi^2}\Big[e^{i\pi x + iKX} + e^{-i\pi x - iKX}\Big]\sin\pi y = \frac{\sqrt{R_2 - 4K^2}}{\pi^2}\cos[(\pi + \epsilon K)x], \tag{4.12}$$

which shows that that wavenumber of the convecting roll has been altered slightly from π.

The presence of the A_{XX} term in the amplitude equation reflects the parabolic nature of the neutral curve near its minimum. The solution (4.12) also shows that $R_2 = 4K^2$ may be regarded as the marginal stability curve — this is consistent with (4.1) above.

4.5. Stability of rolls to sideband disturbances.

The small amplitude of the solution given by (4.12) when R_2 is close to $4K^2$ suggests that it may be possible for such a roll to be unstable to disturbances of the form of a different roll whose wavenumber is closer to π. Such disturbances are called **sideband disturbances** and the instability mechanism is the **Eckhaus instability**.

If we were to linearise equation (4.10) about the solution (4.11), then the introduction of a disturbance which is proportional to $\exp[i(K+L)X]$ yields a term which is proportional to $\exp[i(K-L)X]$, and vice versa. Therefore we need to use two disturbances for this analysis. If we set

$$A = \sqrt{R_2 - 4K^2}e^{iKX} + B_1 e^{i(K+L)X+\lambda\tau} + \bar{B}_2 e^{i(K-L)X+\lambda\tau}, \tag{4.13}$$

and linearise with respect to B_1 and B_2, then we obtain the determinantal equation which must be satisfied if nonzero solutions are required,

$$\begin{vmatrix} R_2 - \lambda - 4(K+L)^2 - 2(R_2 - 4K^2) & -(R - 4K^2) \\ -(R - 4K^2) & R_2 - \lambda - 4(K-L)^2 - 2(R_2 - 4K^2) \end{vmatrix} = 0. \tag{4.14}$$

On setting $\lambda = 0$ this determinant reduces to

$$R = 12K^2 - 2L^2 \tag{4.15}$$

with $\lambda > 0$ for values of R_2 which are smaller than $12K^2 - 2L^2$. The region of instability is maximised by taking the limit $L \to 0$, and therefore the stability criterion for the Eckhaus instability is that

$$R_2 > 12K^2, \tag{4.15}$$

which should be compared with the region of existence of rolls, $R_2 > 4K^2$.

5. Cross-roll instability

In this section we will deal with the instability of the basic roll with respect to roll disturbances aligned at a finite nonzero angle, ϕ, away from the basic roll. As the resulting flow no longer remains two-dimensional, it is necessary to rework the stability analysis in an alternative form. We will use a pressure/temperature formulation.

5.1. Perturbation Equations.

To recap, the basic equations are

$$u_x + v_y + w_z = 0, \tag{5.1a}$$

$$u = -p_x, \qquad v = -p_y + R\theta, \qquad w = -p_z, \tag{5.1b,c,d}$$

$$\theta_t + u\theta_x + v\theta_y + w\theta_z = \nabla^2\theta, \tag{5.1e}$$

subject to the boundary conditions,

$$y = 0: \quad \theta = 1,\ v = 0, \qquad y = 1: \quad \theta = 0,\ v = 0. \tag{5.1f}$$

On elimination of the velocities from (5.1) we obtain the pressure/temperature formulation:

$$\nabla^2 p = R\theta_y, \qquad \theta_t + R\theta\theta_y - \nabla p.\nabla\theta = \nabla^2\theta, \tag{5.2a,b}$$

subject to

$$y = 0: \quad \theta = 1,\ p_y = R, \qquad y = 1: \quad \theta = 0,\ p_y = 0. \tag{5.2c}$$

The conduction solution is easily found to be

$$\theta = 1 - y, \qquad p = R(y - \tfrac{1}{2}y^2) + \text{constant}. \tag{5.3}$$

It is more convenient, in terms of derivation, to work with perturbations with respect to this solution, and therefore we set

$$\theta = 1 - y + \Theta, \qquad p = R(y - \tfrac{1}{2}y^2) + \text{constant} + P. \tag{5.4}$$

into equations (5.2). After dropping the asterisks, we obtain

$$\nabla^2 P = R\Theta_y, \qquad \Theta_t + R\Theta\Theta_y - \nabla P.\nabla\Theta = \nabla^2\Theta + R\Theta - P_y, \tag{5.5a,b}$$

subject to the homogeneous boundary conditions,

$$y = 0: \quad \Theta = 0,\ P_y = 0, \qquad y = 1: \quad \Theta = 0,\ P_y = 0. \tag{5.5c}$$

5.2. Weakly nonlinear expansion.

The weakly nonlinear theory is undertaken in the usual way by setting,

$$\begin{pmatrix} P \\ \Theta \end{pmatrix} = \epsilon \begin{pmatrix} p_1 \\ \theta_1 \end{pmatrix} + \epsilon^2 \begin{pmatrix} p_2 \\ \theta_2 \end{pmatrix} + \cdots, \tag{5.6a}$$

$$R = R_0 + \epsilon^2 R_2 + \cdots, \qquad \tau = \tfrac{1}{2}\epsilon^2 t. \tag{5.6c,d}$$

where $\epsilon \ll 1$ in magnitude. Substitution into (5.5) yields systems of equations at each order in ϵ.

At $O(\epsilon)$ we obtain,

$$\nabla^2 p_1 = R_0\theta_{1y}, \qquad \nabla^2\theta_1 = p_{1y} - R_0\theta_1. \tag{5.7a,b}$$

We remain interested in stability at the bottom of the neutral curve for which the horizontal wavenumber is π and the critical Rayleigh number is $4\pi^2$. Therefore we may use the following as an eigensolution of the homogeneous system (5.7),

$$p_1 = -\frac{1}{\pi}\left[Ae^{i\pi x} + \bar{A}e^{-i\pi x}\right]\cos\pi y, \tag{5.8a}$$

$$\theta_1 = \frac{1}{2\pi^2}\left[Ae^{i\pi x} + \bar{A}e^{-i\pi x}\right]\sin\pi y, \tag{5.8b}$$

$$R_0 = 4\pi^2. \tag{5.8c}$$

Here we assume that $A = A(\tau)$ only and we will delay consideration of slow x-variations using $X = \epsilon^2 x$ until §5.4. However, we are interested in the stability of one roll with respect to disturbances in the form of another roll aligned at a relative angle of ϕ, and therefore we use

$$p_1 = -\frac{1}{\pi}\left[Ae^{i\pi x} + \bar{A}e^{-i\pi x}\right]\cos\pi y - \frac{1}{\pi}\left[Be^{i\pi(x\cos\phi - z\sin\phi)} + \bar{B}e^{-i\pi(x\cos\phi - z\sin\phi)}\right]\cos\pi y, \tag{5.9a}$$

$$\theta_1 = \frac{1}{2\pi^2}\left[Ae^{i\pi x} + \bar{A}e^{-i\pi x}\right]\sin\pi y + \frac{1}{2\pi^2}\left[Be^{i\pi(x\cos\phi - z\sin\phi)} + \bar{B}e^{-i\pi(x\cos\phi - z\sin\phi)}\right]\sin\pi y, \tag{5.9b}$$

instead of (5.8a,b) Note that these A and B components represent precisely the same form of solution as one another, except for the fact that they are aligned at different angles.

At $O(\epsilon^2)$ the equations for p_2 and θ_2 are

$$\nabla^2 p_2 - R_0\theta_{2y} = 0, \tag{5.10a}$$

$$\nabla^2\theta_2 + R_0\theta_2 - p_{2y} = R_0\theta_1\theta_{1y} - \nabla p_1.\nabla\theta_1. \tag{5.10b}$$

The inhomogeneous terms in (5.10b) expand into many lines, and these are omitted for the sake of brevity. The full solutions for p_2 and θ_2 are

$$\begin{aligned} p_2 = {} & \frac{1}{2\pi^2}\left[A\bar{A} + B\bar{B}\right]\cos 2\pi y \\ & + \frac{1}{\pi^2}\frac{(1-\cos\phi)}{(\cos^2\phi + 4\cos\phi + 7)}\left[ABe^{i\pi(x(1+\cos\phi) - z\sin\phi)} + \bar{A}\bar{B}e^{-i\pi(x(1+\cos\phi) - z\sin\phi)}\right]\cos 2\pi y \\ & + \frac{1}{\pi^2}\frac{(1+\cos\phi)}{(\cos^2\phi - 4\cos\phi + 7)}\left[A\bar{B}e^{i\pi(x(1-\cos\phi) + z\sin\phi)} + \bar{A}Be^{-i\pi(x(1-\cos\phi) + z\sin\phi)}\right]\cos 2\pi y \end{aligned} \tag{5.11a}$$

$$\begin{aligned} \theta_2 = {} & -\frac{1}{4\pi^3}\left[A\bar{A} + B\bar{B}\right]\sin 2\pi y \\ & + \frac{1}{4\pi^3}\frac{(\cos^2\phi + 2\cos\phi - 3)}{(\cos^2\phi + 4\cos\phi + 7)}\left[ABe^{i\pi(x(1+\cos\phi) - z\sin\phi)} + \bar{A}\bar{B}e^{-i\pi(x(1+\cos\phi) - z\sin\phi)}\right]\sin 2\pi y \\ & + \frac{1}{4\pi^3}\frac{(\cos^2\phi - 2\cos\phi - 3)}{(\cos^2\phi - 4\cos\phi + 7)}\left[A\bar{B}e^{i\pi(x(1-\cos\phi) + z\sin\phi)} + \bar{A}Be^{-i\pi(x(1-\cos\phi) + z\sin\phi)}\right]\sin 2\pi y \end{aligned} \tag{5.11b}$$

We note that these solutions are valid for all possible angles, ϕ. It might be thought that the value $\phi = \frac{1}{3}\pi$ would cause difficulties since the overall wavenumber of the $A\bar{B}$ terms above is π, the resonant wavelength. However, the y-dependent part of the inhomogeneous terms in (5.10b) is $\sin 2\pi y$, which is a different Fourier component from the resonant $\sin\pi y$ component given in (5.8b). Thus the forcing terms in (5.10b) are always nonresonant, which is confirmed by the fact that the solutions (5.11) are regular for all ϕ.

At $O(\epsilon^3)$ the equations are

$$\nabla^2 p_3 - R_0\theta_{3y} = R_2\theta_{1y} \tag{5.12a}$$

$$\nabla^2\theta_2 + R_0\theta_3 - p_{3y} = R_0(\theta_1\theta_{2y} + \theta_2\theta_{1y}) - \nabla p_1.\nabla\theta_2 - \nabla p_2.\nabla\theta_1 + \tfrac{1}{2}\theta_{1\tau} - R_2\theta_1. \tag{5.12b}$$

As usual, we obtain a time derivative term and a term involving R_2 at this stage, together with nonlinear resonant forcing terms. The nonlinear terms in (5.12b) contain many componants which are nonresonant, and therefore solutions corresponding to those may be obtained if one had the need, the will and the time. However, our aim here is to find a condition which guarantees a solution for the system, and which, therefore, renders the inhomogeneities nonresonant overall. Such a solvability condition is the following.

$$\int\int\int_0^1 \left[\hat{p}_1\mathcal{R}_1 - R_0\hat{\theta}_1\mathcal{R}_2\right] dy\,dx\,dz = 0. \tag{5.13}$$

This condition needs to be applied twice, once for the A-roll and once for the B-roll. In the case of the A-roll we set

$$\hat{p}_1 = -\frac{2}{\pi^2}\bar{A}e^{-i\pi x}\cos\pi y, \tag{5.14a}$$

$$\hat{\theta}_1 = \frac{1}{\pi^2}\bar{A}e^{-i\pi x}\sin\pi y, \tag{5.14b}$$

and take $\mathcal{R}_1$ and $\mathcal{R}_2$ to be those inhomogeneous terms in (5.12a) and (5.12b), respectively, which are proportional to $e^{i\pi x}$ only. Then the integration in (5.13) takes place over one wavelength of the convective roll. For the A-roll we obtain the following for $\mathcal{R}_1$ and $\mathcal{R}_2$:

$$\mathcal{R}_1 = \tfrac{1}{2}R_2 Ae^{i\pi x}\cos\pi y, \tag{5.15a}$$

$$\mathcal{R}_2 = \frac{1}{4\pi^2}A_\tau - \frac{R_2}{2\pi^2}A + \frac{1}{4\pi^2}A^2\bar{A} + \frac{1}{4\pi^2}\left(\frac{70 + 28\cos^2\phi - 2\cos^4\phi}{49 - 2\cos^2\phi + \cos^4\phi}\right)AB\bar{B}. \tag{5.15b}$$

Application of the solvability condition for A now gives

$$A_\tau = R_2 A - \left[A^2\bar{A} + \left(\frac{70 + 28\cos^2\phi - 2\cos^4\phi}{49 - 2\cos^2\phi + \cos^4\phi}\right)AB\bar{B}\right] \tag{5.16a}$$

$$B_\tau = R_2 B - \left[B^2\bar{B} + \left(\frac{70 + 28\cos^2\phi - 2\cos^4\phi}{49 - 2\cos^2\phi + \cos^4\phi}\right)BA\bar{A}\right]. \tag{5.16b}$$

The coupling coefficient, $\Omega(\phi)$, is defined by

$$\Omega(\phi) = \frac{70 + 28\cos^2\phi - 2\cos^4\phi}{49 - 2\cos^2\phi + \cos^4\phi}, \tag{5.17}$$

varies from 2 down to $\frac{10}{7}$; this latter value has great importance in view of the stability characteristics of the convective flow, as will now be demonstrated.

5.3. Basic stability analysis of rolls.

Equations (5.16) have an infinite number of solutions since, for every solution which exists, a similar one with a different phase may be obtained by changing, say, A to $Ae^{i\Phi}$. However, there are three main solutions for which A and B are real and nonnegative. They are

$$A = R_2^{1/2}, \qquad B = 0, \tag{5.18a}$$

$$A = 0, \qquad B = R_2^{1/2}, \tag{5.18b}$$

and

$$A = B = \left(\frac{R_2}{1+\Omega(\phi)}\right)^{1/2}. \tag{5.18c}$$

Before analysing stability, it is instructive to consider the mean rate of heat transfer across the layer for each solution. From equation (5.11b) we see that the *mean* rate of heat transfer is proportional to $(A\bar{A} + B\bar{B})$, and therefore the three solutions given in (5.18) yield values which are proportional to

$$\text{(a)} \quad R_2, \qquad \text{(b)} \quad R_2, \qquad \text{(c)} \quad \frac{2R_2}{1+\Omega(\phi)}. \tag{5.19}$$

Thus the single-roll solutions, (a) and (b), have a higher rate of heat transfer when $\Omega > 1$, but the mixed mode solution transfers a greater amount of heat when $\Omega < 1$. For the present flow Ω is always greater than or equal to $\frac{10}{7}$, and therefore single rolls are favoured from the point of view of heat transfer.

Consider the stability of the single-roll solution given by (5.18a). Let

$$A = R_2^{1/2} + \delta A, \qquad B = \delta B \tag{5.20}$$

in equations (5.16) and linearise with respect to δA and δB. We obtain the linearised disturbance equations,

$$\delta A_\tau = -R_2(\delta A + \delta\bar{A}), \qquad \delta B_\tau = (1-\Omega)R_2\delta B. \tag{5.21a,b}$$

The equation for δA is a little unusual, but if we split δA into its component real and imaginary parts using $\delta A = \delta A_R + i\delta A_I$ we get

$$\delta A_{R\tau} = -2R_2\delta A_R, \qquad \delta A_{I\tau} = 0. \tag{5.22a,b}$$

The equation for δA_R yields an exponentially decaying solution, and therefore the solution (5.18a) is stable with respect to real perturbations in A. The equation for δA_I gives δA_I to be equal to a constant. Therefore if A is perturbed in terms of its imaginary part, then that perturbation remains, and neither grows nor decays. Therefore A is neutrally stable with respect to phase perturbations. Finally, the equation for δB has a decaying solution only when $\Omega > 1$. Therefore in cases like the present, for which Ω is always greater than 1, the roll solution corresponding to the critical wavenumber is always stable. But conversely, for fluid problems where the minimum value of Ω is less than 1, then the mixed mode solution (5.18c) becomes stable, and single rolls are unstable — see §10, for example.

5.4. The effect of small wavenumber variations.

Although we have not yet included small wavenumber changes within the pressure/temperature analysis, the result of doing so for the A-roll yields the same amplitude equation as was obtained using the two-dimensional streamfunction/temperature formulation. Thus A would satisfy

$$A_\tau = R_2 A + 4A_{XX} - A^2\bar{A} - \Omega(\phi)AB\bar{B}. \tag{5.23}$$

The phase-winding solution for A (which replaces (5.18a)), is now

$$A = (R_2 - 4K^2)^{1/2}e^{iKX}, \qquad B = 0. \tag{5.24}$$

For this solution the equation for δB becomes,

$$\delta B_\tau = [R_2(1 - \Omega(\phi)] + K^2\Omega(\phi)]\delta B \tag{5.25}$$

from which we see that we have instability whenever

$$R_2 < \frac{4\Omega}{\Omega - 1}K^2. \tag{5.26}$$

For the present problem the right hand side is maximised by $\phi = \frac{1}{2}\pi$ and therefore the stability region is

$$R_2 = \tfrac{40}{3}K^2. \tag{5.27}$$

which is more restrictive than the Eckhaus instability ($R_2 < 12K^2$). It is usual that the roll at 90° is the most dangerous disturbance, and this is why the instability is called the cross-roll instability.

6. The zigzag instability

The zigzag instability is so-called because when it is operative the cell boundaries, as viewed from above, appear to form slow sinusoidal deformations before eventually becoming a single roll inclined at a very small angle to the original direction with a slightly different wavenumber.

6.1. Reason for the existence of the instability.

When the wavenumber of a roll is slightly less than π, i.e. of the form $k = \pi + \epsilon K$ where K is negative, then it is possible to introduce a small z-component to make the overall wavenumber equal to π. To fix ideas, suppose the original roll were to correspond to the horizontal planform, $\exp[i(\pi + \epsilon K)x]$, then the wavenumber is simply $(\pi + \epsilon K)$. If now the roll has the planform

$$\exp[i(\pi + \epsilon K)x + iM\epsilon^{1/2}z] \tag{6.1}$$

then the overall avenumber is

$$\begin{aligned} k &= \sqrt{(\pi + \epsilon K)^2 + (M\epsilon^{1/2})^2} \\ &= \sqrt{\pi^2 + (2\pi K + M^2)\epsilon + \cdots} \\ &= \pi + \left(K + \frac{M^2}{2\pi}\right)\epsilon + \cdots. \end{aligned} \tag{6.2}$$

Thus the $O(\epsilon)$ correction to π disappears when

$$M = \sqrt{-2\pi K}. \tag{6.3}$$

And therefore a roll with planform (6.1) where M is given by (6.3) has wavenumber equal to π, at least to $O(\epsilon)$, and is inclined at an $O(\epsilon^{1/2})$ angle to the orginal roll. This suggests that we now introduce a slow spatial scale in the z-direction.

6.2. Weakly nonlinear analysis.

Unfortunately the analysis remains three-dimensional, and therefore it is still essential to use the pressure/temperature formulation, but we need only consider a single roll. Therefore we use the slow spatial variables

$$X = \epsilon x \qquad Z = \epsilon^{1/2} z, \tag{6.4}$$

and use the method of multiple scales. As for the Eckhaus instability we make the following replacements

$$\frac{\partial}{\partial x} \quad \rightarrow \quad \frac{\partial}{\partial x} + \epsilon\frac{\partial}{\partial X}, \qquad \text{and} \qquad \frac{\partial^2}{\partial x^2} \quad \rightarrow \quad \frac{\partial^2}{\partial x^2} + 2\epsilon\frac{\partial^2}{\partial x \partial X} + \epsilon^2\frac{\partial^2}{\partial X^2}. \tag{6.5}$$

But since the roll we will be considering is not dependent on z except on the long length scale represented by Z we may use a straightforward transformation from z to Z using

$$\frac{\partial}{\partial z} \quad = \quad \epsilon\frac{\partial}{\partial Z} \qquad \text{and} \qquad \frac{\partial^2}{\partial z^2} \quad = \quad \epsilon^2\frac{\partial^2}{\partial Z^2}. \tag{6.6}$$

Therefore the perturbation equations given by (5.5a,b) become,

$$\nabla^2 p - R_0\theta_y = \epsilon^2 R_2\theta_y - \epsilon(2p_{xX} + p_{ZZ}) - \epsilon^2 p_{XX}, \tag{6.7a}$$

$$\begin{aligned} \nabla^2\theta = {} & p_y - (R_0 + \epsilon^2 R_2)\theta \\ & - \epsilon(2\theta_{xX} + \theta_{ZZ}) - \epsilon^2\theta_{XX} \\ & - \nabla p.\nabla\theta - \epsilon(p_x\theta_X + p_X\theta_x + p_Z\theta_Z) - \epsilon^2 p_X\theta_X \end{aligned} \tag{6.7b}$$

At $O(\epsilon)$ we obtain the equations (5.7) for which the solution is

$$p_1 = -\frac{1}{\pi}\Big[Ae^{i\pi x} + \bar{A}e^{-i\pi x}\Big]\cos\pi y, \tag{6.8a}$$

$$\theta_1 = \frac{1}{2\pi^2}\Big[Ae^{i\pi x} + \bar{A}e^{-i\pi x}\Big]\sin\pi y, \tag{6.8b}$$

where A is now a function of τ, X and Z.

At $O(\epsilon^2)$ the equations are

$$\begin{aligned}\nabla^2 p_2 - R_0\theta_{2y} &= -2p_{1xX} - p_{1ZZ}\\ &= 2i\pi\Big[A_X e^{i\pi x} - \bar{A}_X e^{-i\pi x}\Big]\cos\pi y + \frac{1}{\pi}\Big[A_{ZZ}e^{i\pi x} + \bar{A}_{ZZ}e^{-i\pi x}\Big]\cos\pi y.\end{aligned} \tag{6.9a}$$

$$\begin{aligned}\nabla^2\theta_2 + R_0\theta_2 - p_{2y} = &-2\theta_{1xX} - \theta_{1ZZ} + R_0\theta_1\theta_{1y} - p_{1x}\theta_{1x} - p_{1y}\theta_{1y}\\ &- \frac{i}{\pi}\Big[A_X e^{i\pi x} - \bar{A}_X e^{-i\pi x}\Big]\sin\pi y\\ &- \frac{1}{2\pi^2}\Big[A_{ZZ}e^{i\pi x} + \bar{A}_{ZZ}e^{-i\pi x}\Big]\sin\pi y + \text{old terms}\end{aligned} \tag{6.9b}$$

Although these new inhomogeneous terms appear to be resonant, the application of the solvability condition shows that the equations are indeed solvable. This may be tested by substituting back into the governing equations (6.9) the following solutions,

$$p_2 = \frac{1}{2\pi^2}A\bar{A}\cos 2\pi y - \frac{1}{4\pi^3}\Big[A_{ZZ}e^{i\pi x} + \bar{A}_{ZZ}e^{-i\pi x}\Big]\cos\pi y - \frac{i}{2\pi^2}\Big[A_X e^{i\pi x} - \bar{A}_X e^{-i\pi x}\Big]\cos\pi y, \tag{6.10a}$$

$$\theta_2 = -\frac{1}{4\pi^3}A\bar{A}\sin 2\pi y - \frac{1}{8\pi^4}\Big[A_{ZZ}e^{i\pi x} + \bar{A}_{ZZ}e^{-i\pi x}\Big]\sin\pi y - \frac{i}{4\pi^3}\Big[A_X e^{i\pi x} - \bar{A}_X e^{-i\pi x}\Big]\sin\pi y. \tag{6.10b}$$

At $O(\epsilon^3)$ we obtain all the right hand sides which appear in equations (5.15), but with the extra terms,

$$\frac{i}{\pi^2}\Big[A_{XXZ}e^{i\pi x} - \bar{A}_{XXZ}e^{-i\pi x}\Big]\cos\pi y + \frac{1}{4\pi^3}\Big[A_{ZZZZ}e^{i\pi x} + \bar{A}_{ZZZZ}e^{-i\pi x}\Big]\cos\pi y \tag{6.11a}$$

in (5.15a) and

$$\begin{aligned}&-\frac{1}{\pi^2}\Big[A_{XX}e^{i\pi x} + \bar{A}_{XX}e^{-i\pi x}\Big]\sin\pi y + \frac{i}{2\pi^3}\Big[A_{XXZ}e^{i\pi x} - \bar{A}_{XXZ}e^{-i\pi x}\Big]\sin\pi y\\ &\quad + \frac{1}{8\pi^4}\Big[A_{ZZZZ}e^{i\pi x} + \bar{A}_{ZZZZ}e^{-i\pi x}\Big]\sin\pi y\end{aligned} \tag{6.11b}$$

in equation (5.15b). Application of the solvability condition now yields

$$A_\tau = R_2 A + 4\Big[A_{XX} - \frac{i}{\pi}A_{XZZ} - \frac{1}{4\pi^2}A_{ZZZZ}\Big] - A^2\bar{A} = 0. \tag{6.12}$$

This may be shortened slightly to the following form,

$$A_\tau = R_2 A + 4\Big[\frac{\partial}{\partial X} - \frac{i}{2\pi}\frac{\partial^2}{\partial Z^2}\Big]^2 A - A^2\bar{A} = 0. \tag{6.13}$$

6.3. Stability analysis.

Now we may proceed to the analysis of the zigzag instability. We perturb about the basic solution, $A = (R_2 - 4K^2)^{1/2}e^{iKX}$, using a pair of rolls with infinitesimal amplitude. Therefore we set

$$A = (R_2 - 4K^2)e^{iKX} + A_1 e^{i[(K+L)X+MZ]} + \bar{A}_2 e^{i[(K-L)X-MZ]} \tag{6.14}$$

into equation (6.13). We eventually obtain the amplitude equations

$$A_{1\tau} = R_2 A_1 - \Big[\frac{M^2}{\pi} + 2(K+L)\Big]^2 A_1 - 2(R_2 - 4K^2)A_1 - (R_2 - 4K^2)A_2, \tag{6.15a}$$

$$A_{2\tau} = R_2 A_2 - \Big[\frac{M^2}{\pi} + 2(K-L)\Big]^2 A_2 - 2(R_2 - 4K^2)A_2 - (R_2 - 4K^2)A_1 \tag{6.15b}$$

for A_1 and A_2. On setting both A_1 and A_2 to be proportional to $\exp(\lambda t)$, the condition for a nonzero solution reduces to the following determinantal equation,

$$\begin{vmatrix} R_2 - \lambda - \Big[\frac{M^2}{\pi} + 2(K+L)\Big]^2 - 2(R_2 - 4K^2) & -(R - 4K^2) \\ -(R - 4K^2) & R_2 - \lambda - \Big[\frac{M^2}{\pi} + 2(K-L)\Big]^2 - 2(R_2 - 4K^2) \end{vmatrix} = 0. \tag{6.16}$$

which clearly reduces to (4.13) when $M = 0$.

We find that

$$\lambda = -\Big[R_2 - 4K^2 + 4L^2 + \frac{4M^2K}{\pi} + \frac{M^4}{\pi^2}\Big] \pm \sqrt{(R_2 - 4K^2)^2 + 16L^2\Big(2K + \frac{M^2}{\pi}\Big)^2}. \tag{6.17}$$

On setting $\partial\lambda/\partial L = 0$ we may maximise the growth rate. This turns out to be when $L = 0$. Hence the above expression for λ reduces to

$$\lambda = -\frac{M^2}{\pi^2}\Big(M^2 + 4K\pi\Big). \tag{6.18}$$

This, in turn, is maximised when

$$M^2 = -2\pi K. \tag{6.19}$$

The expression (6.18) is positive only when $K < 0$, and whenever $K < 0$ we can obtain a value for M for which the roll is unstable. Therefore the stability criterion is that $K > 0$ for stability.

6.4. Concluding remarks.

We have considered three instability mechanisms for the roll $A = \sqrt{R_2 - 4K^2}e^{iKX}$. The Eckhaus instability is operative when $R_2 < 12K^2$, the cross-roll instability when $R_2 < \frac{40}{3}K^2$ (which is more restrictive in terms of the region of stability), and the zigzag instabity when $K < 0$. When other effects are included then these neutral curves are modified and their relative importances are also changed.

7. Weak imperfections: form drag

In §2.2 we presented the linearised analysis of the effect of form drag on the onset criterion and found that there is no effect. Now we will consider weakly nonlinear convection for it is to be expected that there will now be an effect since there exists convection at supercritical Rayleigh numbers.

7.1. Weakly nonlinear analysis.

The full perturbation equations are given by

$$(1+Gq)(\Psi_{xx}+\Psi_{yy})+G(\Psi_x q_x+\Psi_y q_y)=R\Theta_x, \tag{7.1}$$

$$\Theta_t-\Psi_x+\Psi_x\Theta_y-\Psi_y\Theta_x=\Theta_{xx}+\Theta_{yy}. \tag{7.2}$$

We will consider the form drag effect to be weak and therefore we set

$$G=G^*\epsilon \tag{7.3}$$

in equation (7.1). The reason for this is that we wish to obtain a form drag modification to the amplitude equation at $O(\epsilon^3)$, and this magnitude for G allows for these effects to arise at that point in the analysis. In their seminal paper He and Georgiadis (1990) considered the combined effects of form drag inertia, internal heating and thermal dispersion, but since the form drag parameter was of $O(1)$ it became essential to apply a solvability condition at $O(\epsilon^2)$, and therefore the cubic nonlinear terms were absent from their amplitude equation. Allowing G to be of $O(\epsilon)$ allows us to investigate the transition from inertia-dominated to inertia-free flow.

We will use the real form of the $O(\epsilon)$ solution given in §3.2 to perform this analysis which will cover only the derivation of the basic amplitude equation. Therefore we take the $O(\epsilon)$ solutions to be

$$\psi_1=\frac{2}{\pi}A\sin\pi x\sin\pi y,\qquad \theta_1=\frac{1}{\pi^2}A\cos\pi x\sin\pi y, \tag{7.4}$$

where $A=A(\tau)$ is a real amplitude.

At $O(\epsilon^2)$ the solution is again

$$\psi_2=0,\qquad \theta_2=-\frac{1}{4\pi^3}A^2\sin 2\pi y. \tag{7.5}$$

At $O(\epsilon^3)$ we obtain a complicated set of equations which we have omitted for the sake of brevity. Application of a solvability condition yields the amplitude equation

$$A_\tau=R_2A-\alpha A|A|-A^3, \tag{7.6}$$

where α is a constant given by

$$\begin{aligned}\alpha&=8\pi^2G^*\int_0^1\int_0^2[\cos^2\pi x\,\sin^2\pi y+\sin^2\pi x\,\cos^2\pi y]^{3/2}\,dx\,dy\\&=0.776534\times 8\pi^2G^*\\&=61.3127G^*.\end{aligned} \tag{7.7}$$

The steady solutions of equation (7.6) are

$$A=\pm\frac{2R_2}{\alpha+[\alpha^2+4R_2)]^{1/2}}, \tag{7.8}$$

a sketch of which is given in Figure 7.1. Here we see that the nonzero solution branches approach the origin at a finite slope, rather than display the square root behaviour which is typical of the classical Darcy flow case which is shown in Figure 3.1. Indeed, if we expand equation (7.8) for small values of R_2, we obtain

$$A = \pm\Big[\frac{R_2}{\alpha} - \frac{R_2^2}{\alpha^3} + \cdots\Big] \tag{7.9}$$

which shows that A has a finite slope at the origin. However, for large values of R_2 we obtain

$$A = \pm\Big[R_2^{1/2} - \tfrac{1}{2}\alpha + \cdots\Big], \tag{7.10}$$

which shows that the usual square-root behaviour is re-established when R_2 is relatively large.

Indeed, this is an unusual result for it seems that form drag effects are most prevalent when the flow is relativly weak. However, intuition guides us correctly if we consider what happens when the inertia parameter, α, increases. The asymptotic form for equation (7.8) as α becomes large is given by (7.9), and therefore, for a fixed value of R_2, convection becomes weaker as the effect of form drag increases.

This analysis, together with a study of the Eckhaus, cross-roll and zigzag instabilities, are given in Rees (1996).

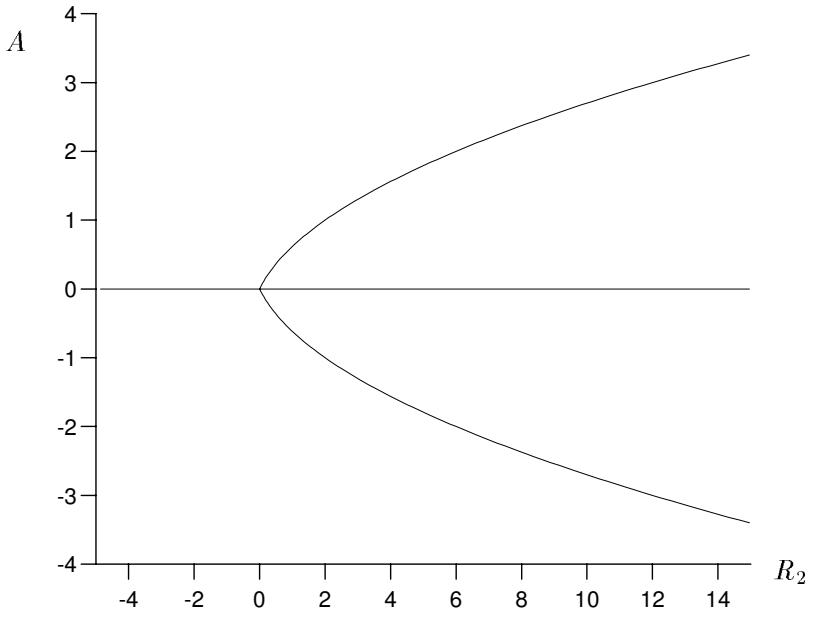

Figure 7.1. Showing the bifurcation diagram for convection in the presence of form drag inertia. The stability characteristics of each branch are the same as for Figure 3.1, but the upper and lower branches have a finite slope at $R_2 = 0$.

8. Weak imperfections: resonant thermal forcing

In this section we consider how a slight change to the boundary temperatures affect the onset of convection. In particular we will assume that the temperatures of the upper and lower surfaces are

$$y = 0: \quad \theta = 1 + \delta \cos \pi x, \qquad y = 1: \quad \theta = \delta \cos \pi x, \tag{8.1}$$

where the amplitude, δ, of the thermal imperfections is very small. We have chosen the symmetry of this imperfection carefully, since it represents the general case for imperfections of this wavenumber — this aspect will be discussed in more detail at the end of the section.

8.1. The basic flow due to the imperfection.

The presence of a nonuniform temperature at the boundary causes fluid motions to exist at all nonzero Rayleigh numbers, therefore it is necessary to determine this flow and temperature field first. As $\delta \ll 1$ we may do this using a perturbation expansion of the form,

$$\begin{pmatrix} \Psi \\ \Theta \end{pmatrix} = \delta \begin{pmatrix} \psi^{(1)} \\ \theta^{(1)} \end{pmatrix} + \delta^2 \begin{pmatrix} \psi^{(2)} \\ \theta^{(2)} \end{pmatrix} + \cdots. \tag{8.3}$$

The equations for $\psi^{(1)}$ and $\theta^{(1)}$ are

$$\nabla^2 \psi^{(1)} - R_0 \theta^{(1)}_x, \qquad \nabla^2 \theta^{(1)} - \psi^{(1)}_x = 0, \tag{8.4}$$

subject to the boundary conditions

$$\psi^{(1)} = 0, \quad \theta^{(1)} = \cos \pi x \quad \text{on} \quad y = 0, 1. \tag{8.5}$$

The solution is

$$\psi^{(1)} = \frac{R^{1/2}}{2} \Big[\frac{\cosh \chi(y - \frac{1}{2})}{\cosh \frac{1}{2}\chi} - \frac{\cosh \gamma(y - \frac{1}{2})}{\cosh \frac{1}{2}\gamma} \Big] \sin \pi x, \tag{8.6a}$$

$$\theta^{(1)} = \frac{1}{2} \Big[\frac{\cosh \chi(y - \frac{1}{2})}{\cosh \frac{1}{2}\chi} + \frac{\cosh \gamma(y - \frac{1}{2})}{\cosh \frac{1}{2}\gamma} \Big] \cos \pi x, \tag{8.6b}$$

where

$$\chi^2 = \pi^2 - \pi R^{1/2} \quad \text{and} \quad \gamma^2 = \pi^2 + \pi R^{1/2}. \tag{8.6c}$$

From this expression for $\theta^{(1)}$ it is possible to find the surface rates of heat transfer, but it is very important to note that both $\psi^{(1)}$ and $\theta^{(1)}$ are singular in the limit $R \to 4\pi^2 = R_c$. That this is so may be seen by considering the denominator,

$$\cosh \tfrac{1}{2}\chi = \cos \Big[\tfrac{1}{2} \sqrt{\pi R^{1/2} - \pi^2} \Big] \qquad \longrightarrow \qquad \cos \tfrac{1}{2}\pi = 0 \quad \text{as} \quad R \to 4\pi^2. \tag{8.7}$$

8.2. Removal of the singularity.

The solution becomes infinite because the thermal forcing at the boundaries becomes resonant as the Rayleigh number tends towards $4\pi^2$. In fact, at $R = 4\pi^2$ no solution exists. This situation is similar to that which arises at $O(\epsilon^3)$ in the above weakly nonlinear analyses where solvability conditions are obtained in order remove the resonance. Therefore, if we are to determine how the present thermal forcing affects the onset of convection, it is necessary to place the forcing effects at $O(\epsilon^3)$ in our analysis. So we will set $\delta = \epsilon^3$, and carry out the weakly analysis in the same way as before.

We will assume that the $O(\epsilon)$ and $O(\epsilon^2)$ solutions given in §3.1–§3.3 are valid here too. At $O(\epsilon^3)$ the equations are given by (3.12):

$$\nabla^2 \psi_3 - R_0 \theta_3 = -\frac{1}{\pi} R_2 A \sin \pi x \sin \pi y, \tag{8.8a}$$

$$\nabla^2\theta_3 - \psi_{3x} = \frac{1}{2\pi^2}A^3\cos\pi x(\sin\pi y - \sin 3\pi y) + \frac{1}{2\pi^2}A_\tau\cos\pi x\sin\pi y, \tag{8.8b}$$

and the boundary conditions by

$$\psi_3 = 0, \quad \theta_3 = \cos\pi x. \tag{8.8c}$$

The sole difference between the present system of equations, (8.8), and those given in §3, (3.12), is that the present boundary conditions for θ_3 are inhomogeneous, whereas the boundary conditions for (3.12) are homogeneous. This means that the solvability condition will be slightly different from what was derived earlier.

Using (3.14) the solvability condition becomes

$$\begin{aligned} I &= \int_0^{2\pi}\int_0^1 \Big[[\nabla^2\psi_3 - R_0\theta_3]\psi_1 + [\nabla^2\theta_3 - \psi_{3x}]R_0\theta_1\Big]\,dy\,dx, \\ &= \int_0^{2\pi}\int_0^1 \Big[[\nabla^2\psi_1 - R_0\theta_1]\psi_3 + [\nabla^2\theta_1 - \psi_{1x}]R_0\theta_3\Big]\,dy\,dx \quad + \quad \frac{2AR_0}{\pi} \\ &= \frac{2AR_0}{\pi}. \end{aligned} \tag{8.9}$$

Hence the solvability condition is

$$I = \int_0^{2\pi}\int_0^1 \Big[\mathcal{R}_1\psi_1 + \mathcal{R}_2\theta_1 R_0\Big]\,dy\,dx = \frac{2AR_0}{\pi}. \tag{8.10}$$

where $\mathcal{R}_1$ and $\mathcal{R}_2$ are the respective right hand sides of equations (8.8a) and (8.8b). After a little more integration we obtain the amplitude equation,

$$A_\tau = R_2 A - A^3 + 8\pi^3. \tag{8.11}$$

A sketch of the steady solutions corresponding to equation (8.11) are given in Figure 8.1. This is an example of an **imperfect bifurcation** where one strongly convecting branch (the upper one here) is connected smoothly to the solution which arises when R_2 is large and negative, and where the other two branches, the lower and middle branches, are now disconnected from the upper branch.

A straightforward analysis of equation (8.11) shows that the subcritical branch and the middle supercritical branch satisfy the relation $A \sim -8/\pi^3/R_2$, while the upper and lower supercritical branches satisfy $A \sim \pm R_2^{1/2}$, which is asymptotically the same as for when the thermal imperfections are absent.

8.3. Stability analysis.

Given that the bifurcation diagram has changed shape from what it was in Figure 3.1, it is worth checking the solutions for stability.

If we assume that $A = A_0$ is a steady solution of equation (8.11), then we may introduce a small perturbation, δA, in the usual way. Therefore we set

$$A = A_0 + \delta A, \tag{8.12}$$

into (8.11) and linearise with respect to δA. The perturbation satisfies

$$\delta A_\tau = (R_2 - 3A_0^2)\delta A. \tag{8.13}$$

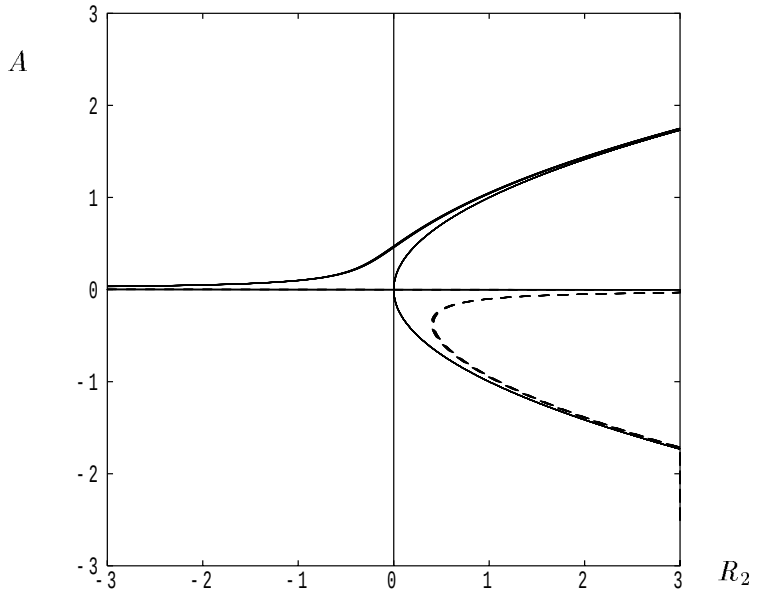

Figure 8.1. Showing the bifurcation diagram for the imperfect bifurcation given by the steady solutions of (8.11). The thick solid lines denote stable solutions, while the dashed lines correspond to unstable solutions. The thin solid lines correspond to the supercritical bifurcation (see Figure 3.1) for comparison.

We have neutral stability when $R_2 = 3A_0^2$, and this occurs when A_0 corresponds to the turning point which separates the lower and the middle branches of Figure 8.1. On the middle branch $R_2 > 3A_0^2$ and therefore this branch is unstable with respect to perturbations in amplitude. But as $R_2 < 3A_0^2$ on the outer branches, this means that they are stable with respect to amplitude perturbations.

We now turn to perturbations in phase. But to do this we must again retrun to the complex form of the amplitude such as we did in §4. Thus if A is now the complex amplitude, equation (8.11) is replaced by

$$A_\tau = R_2 A - A^2 \bar{A} + 8\pi^3. \tag{8.14}$$

If we again perturb according to (8.12), but allow δA to be complex, then δA satisfies

$$\delta A_\tau = (R_2 - 2A_0^2)\delta A - A_0^2 \delta \bar{A}. \tag{8.15}$$

We split δA into its real and imaginary components: $\delta A = \delta A_r + i\delta A_i$, and substitute into equation (8.15) to obtain

$$\delta A_{r\tau} = (R_2 - 3A_0^2)\delta A_r, \qquad \delta A_{i\tau} = (R_2 - A_0^2)\delta A_i. \tag{8.16a,b}$$

Clearly (8.16a) is identical to (8.13). Perturbations with respect to phase may be seen to be stable when $R_2 < A_0^2$, and this occurs only for the upper branch. However, $R_2 > A_0^2$ on the lower branch, and this means that it is unstable with respect to phase perturbations.

This result may be interpreted physically by first noting that the thermal imperfections on the boundary cause the fluid to circulate in one particular way, and since the upper branch is connected to the subcritical branch, the upper branch represents the natural direction of flow. However, the bifurcation diagram clearly shows that it is possible to have circulations in exactly

the opposite sense and this corresponds to the lower branch. But it is unstable, and if it suffers a perturbation with respect to its phase (i.e. its position relative to the thermal forcing) then the perturbation will grow and the rolls will migrate towards the position corresponding to the upper branch.

This work was presented in Rees and Riley (1986), although it should be noted that a slightly more general problem was considered in that paper, and that the nondimensionalisation used there was different.

9. Weak imperfections: internal heating

9.1. Perturbation equations.

We will now modify the classical Darcy-Bénard problem by introducing weak internal heating. The main effect of this modification to note at this stage is the fact that the basic temperature profile does not remain antisymmetric about the centre of the channel. This eventually has important ramifications for the weakly nonlinear theory. First, the presence of these imperfections serves to change the critical Rayleigh number slightly. Secondly, it alters completely the character of the flow near $R = R_c$ by making it three-dimensional. The present analysis has not yet appeared in the research literature.

The basic three-dimensional equations are given by

$$\nabla^2 p = R\theta_y, \qquad \theta_t + R\theta\theta_y - \nabla p.\nabla\theta = \nabla^2\theta + \epsilon. \tag{9.1a,b}$$

The final term in equation (9.1b) represents the effect of internal heating, and we will assume that ϵ is small in magnitude in order to perform a slightly modified weakly nonlinear analysis. The basic temperature and pressure fields are given by

$$\theta = 1 - y + \epsilon\Big(\frac{y - y^2}{2}\Big), \qquad p_y = R\theta. \tag{9.2}$$

If we now perturb about this solution in the usual way we obtain

$$\nabla^2 P = R\Theta_y, \qquad \Theta_t + R\Theta\Theta_y - \nabla P.\nabla\Theta + [-1 + \epsilon(\tfrac{1}{2} - y)][R\Theta - P_y] = \nabla^2\Theta, \tag{9.3a,b}$$

which is subject to $P_y = \Theta = 0$ on $y = 0, 1$.

9.2. The $O(\epsilon)$ solutions.

At $O(\epsilon)$ we recover equations (5.7), but, instead of assuming a solution in the form of two rolls, we will take three rolls at an angle of 60° to each other. Therefore we take

$$p_1 = -\frac{1}{\pi}\cos\pi y\Big[Ae^{i\pi x} + Be^{i\pi(x-\sqrt{3}z)/2} + Ce^{i\pi(x+\sqrt{3}z)/2} + c.c.\Big], \tag{9.4a}$$

$$\theta_1 = \frac{1}{2\pi^2}\sin\pi y\Big[Ae^{i\pi x} + Be^{i\pi(x-\sqrt{3}z)/2} + Ce^{i\pi(x+\sqrt{3}z)/2} + c.c.\Big], \tag{9.4b}$$

where "c.c." stands for "complex conjugate", for convenience. Here the amplitudes, A, B and C, are functions of τ only.

9.3. The $O(\epsilon^2)$ solutions..

Clearly the solutions at this order are particularly lengthy to present, but the extra terms which take the same form as those given in (5.11) may be determined easily simply by associating coefficients with certain overall wavenumbers. However, the presence of the extra ϵ terms in equations (9.3) gives rise to further forcing terms which were not present in the analysis of §5. If we neglect the forcing terms shown in (5.10), just for clarity of presentation, then we need to solve the system,

$$\nabla^2 p_2 - R_0\theta_{2y} = 0, \tag{9.5a}$$

$$\nabla^2\theta_2 + R_0\theta_2 - p_{2y} = \tfrac{1}{2}(1 - 2y)\sin\pi y\Big[Ae^{i\pi x} + Be^{i\pi(x-\sqrt{3}z)/2} + Ce^{i\pi(x+\sqrt{3}z)/2} + c.c.\Big], \tag{9.5b}$$

These terms appear to be resonant, given their horizontal wavenumber, but they are antisymmetric in the y-direction, and therefore it is possible to solve the system. After much algebra we find that the extra solutions at this order are

$$\begin{pmatrix} p_2 \\ \theta_2 \end{pmatrix} = \begin{pmatrix} F_p(y) \\ G_p(y) \end{pmatrix}\Big[Ae^{i\pi x} + Be^{i\pi(x-\sqrt{3}z)/2} + Ce^{i\pi(x+\sqrt{3}z)/2} + c.c.\Big], \tag{9.6}$$

where

$$F_p(y) = -\tfrac{1}{4}(y-y^2)\sin\pi y + \frac{3}{2\pi^2}\sin\pi y + \frac{\sqrt{3}}{\pi^2}\frac{\cosh\sqrt{3}\pi(y-\frac{1}{2})}{\sinh\frac{1}{2}\sqrt{3}\pi}, \tag{9.7a}$$

$$G_p(y) = -\frac{1}{8\pi}(y-y^2)\cos\pi y + \frac{1}{8\pi^3}\cos\pi y + \frac{1}{8\pi^3}\frac{\sinh\sqrt{3}\pi(y-\frac{1}{2})}{\sinh\frac{1}{2}\sqrt{3}\pi}. \tag{9.7b}$$

9.4. The extra terms at $O(\epsilon^3)$.

There are two sets of extra terms which arise at this order. The first set are linear in the amplitudes, but the second are quadratic. The first set of extra terms appear on the right hand side of the equation (5.12b) and are

$$(\tfrac{1}{2}-y)\Big[R_0\theta_2 - p_{2y}\Big] = (\tfrac{1}{2}-y)\Big[R_0G_p - F_p'\Big]\Big[Ae^{i\pi x} + Be^{i\pi(x-\sqrt{3}z)/2} + Ce^{i\pi(x+\sqrt{3}z)/2} + c.c.\Big] \tag{9.8}$$

The application of the solvability condition, as described in §5.2, yields a term which is proportional to either A, B or C, depending on which mode is being considered.

The second set of extra terms arise from the nonlinear interaction of the new $O(\epsilon^2)$ solutions with the $O(\epsilon)$ rolls. Specifically, we are considering

$$R_0[\theta_1\theta_{2y} + \theta_2\theta_{1y}] - \nabla p_1.\nabla\theta_2 - \nabla p_2.\nabla\theta_{1y}, \tag{9.9}$$

where p_1 and θ_1 are given in (9.4) and p_2 and θ_2 are the new $O(\epsilon^2)$ solutions given by (9.6). Again, these products expand into many lines, but most of the resulting terms are nonresonant because the horizontal wavenumber is not equal to π. However, the following are those terms which are resonant:

$$\Big[3G_p'\sin\pi y + 5\pi G_p\cos\pi y - \tfrac{1}{2}F_p\sin\pi y - \tfrac{1}{2\pi}F_p'\cos\pi y\Big]\times$$

$$\Big[BCe^{i\pi x} + A\bar{C}e^{i\pi(x-\sqrt{3}z)/2} + A\bar{B}e^{i\pi(x+\sqrt{3}z)/2} + c.c.\Big]. \tag{9.10}$$

Once more, these terms may be added into the solvability condition in the usual way.

The end result of dealing with this complexity is the following system of amplitude equations,

$$A_\tau = (R_2 - R_h)A - A^2\bar{A} - \Omega(\tfrac{1}{3}\pi)A(B\bar{B} + C\bar{C}) + HBC, \tag{9.11a}$$

$$B_\tau = (R_2 - R_h)B - B^2\bar{B} - \Omega(\tfrac{1}{3}\pi)B(A\bar{A} + C\bar{C}) + HA\bar{C}, \tag{9.11b}$$

$$C_\tau = (R_2 - R_h)C - C^2\bar{C} - \Omega(\tfrac{1}{3}\pi)C(A\bar{A} + B\bar{B}) + HA\bar{B}, \tag{9.11c}$$

where

$$\Omega(\tfrac{1}{3}\pi) = \frac{410}{259} = 1.58301. \tag{9.12}$$

The constants, H and R_h, have not yet been computed. The value R_h represents the change in the critical Rayleigh number of a single roll due to the internal heating effect. The value H represents the interaction of two of the rolls to form a disturbance in the form of the third roll, and this is mediated by the slightly modified symmetry of the basic temperature profile.

9.5. Solutions of the amplitude equation.

While it is possible to obtain single roll solutions such as, $A = \sqrt{R_2 - R_h}$, $B = C = 0$, it is the purpose of this section to consider the resulting three-dimensional solution when A, B and C are all nonzero.

Given the inherent symmetry of the system (9.12), it is to be expected that a solution satisfying $A = B = C$ exists. If we assume this, then we obtain

$$A = B = C = \frac{H \pm \sqrt{H^2 + 4(R_2 - R_h)(1 + 2\Omega)}}{2(1 + 2\Omega)}. \tag{9.13}$$

This solution will appear in practice as a hexagonal pattern of convection. A sketch of the bifurcation diagram is given in Figure 9.1.

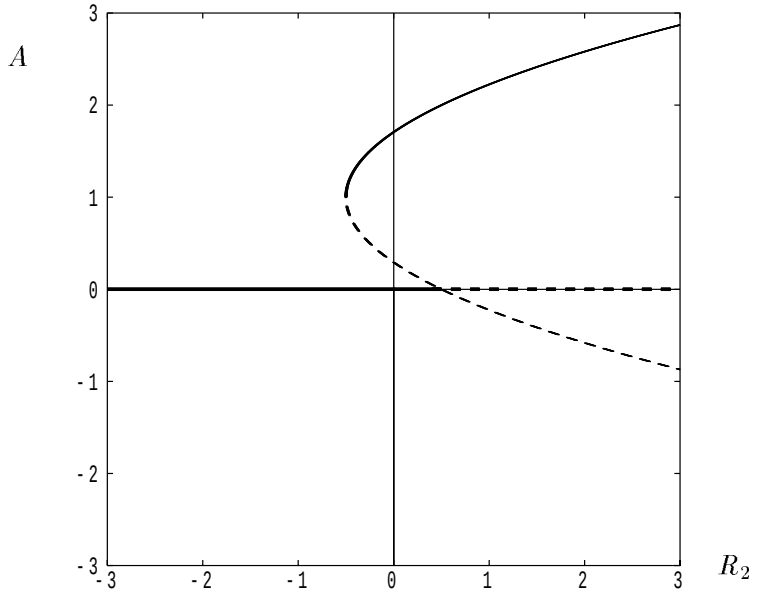

Figure 9.1. Showing the bifurcation diagram for the transcritical bifurcation given by the steady solutions of (9.11) with $A = B = C$. The solid lines denote stable solutions, while the dashed lines correspond to unstable solutions.

The bifurcation from $A = 0$ which takes place at $R_2 = R_h$ is called a **transcritical bifurcation**. The minimum value of R_2 on the curve may be shown to be

$$R_2 = R_h - \frac{H^2}{4(1 + 2\Omega)}, \tag{9.14}$$

at which point

$$A = \frac{H}{2(1 + 2\Omega)}. \tag{9.15}$$

This point is called a **turning point**. Although we do not present a stability analysis of the various branches of the solution, their stability is indicated in Figure 9.1. Of great interest is the fact that this diagram suggests that hysteresis is possible. Thus if we have a zero solution at a strongly negative value of R_2, then it becomes unstable when R_2 is raised to a value above R_h, and grows towards the upper branch. If, subsequently, R_2 is lowered, then the finite amplitude solution will persist until R_2 is less than the value given in (9.14). This is one example of a stability problem where the linearised theory (which predicts onset at $R_2 = R_h$) gives misleading information. So we find that flow may occur at values of R_2 which are subcritical from the point of view of linearised theory.

Finally we need to comment on the instability of the upper branch of Figure 9.1. A detailed linear stability analysis of hexagons on this branch reveals that once R_2 is sufficiently high, then

the flow becomes unstable and it will eventually evolve back into the more usual single-roll. That this is reasonable may be inferred from the behaviour of the mean heat transfer due to the hexagonal pattern,

$$A\bar{A} + B\bar{B} + C\bar{C} = 3\Big[\frac{H + \sqrt{H^2 + 4(R_2 - R_h)(1 + 2\Omega)}}{2(1 + 2\Omega)}\Big]. \tag{9.16}$$

as compared with that for a single roll,

$$A\bar{A} = R_2. \tag{9.17}$$

These rates of heat transfer are equal when

$$R_2 = R_h + \frac{3H^2}{4(\Omega - 1)^2}. \tag{9.18}$$

When R_2 is higher than this value, then single rolls transport more heat than do hexagons.

10. Strong imperfections: finite conductivity effects

In all the problems considered so far the upper and lower surfaces of the layer have had a temperature or temperature distribution imposed upon them. In the section we will relax this assumption by allowing the porous layer to be sandwiched between two semi-infinite conducting but impermeable regions. This set-up may be regarded as applying to a layer of porous rock placed between two impermeable rocks. The following will give an extremely brief summary of the results of the paper by Riahi (1983); the detailed analysis follows that of §5, and therefore it is not necessary to repeat it here.

10.1. Boundary conditions.

We will denote by θ_t the temperature field in the impermeable region above the porous layer and by θ_b the temperature in the region below below the layer. The $y = 0$ boundary condition for θ, the temperature of the porous medium, is given by

$$\theta = \theta_b, \qquad \theta_y = \gamma_b \theta_{by}, \tag{10.1a}$$

and, at $y = 1$

$$\theta = \theta_t, \qquad \theta_y = \gamma_t \theta_{ty}. \tag{10.1b}$$

The presence of these finitely conducting regions will alter the boundary conditions used to solve all the intermediate equations considered in §5, although the equations themselves remain unaltered. Riahi (1983) also showed how to take account of the conduction field in the upper and lower regions by modifying the above boundary conditions. So, for example, if the convective cells in the porous layer have wavenumber k, then (10.1a,b) are replaced by

$$y = 0: \quad \theta_y = k\gamma_b \theta \qquad\qquad y = 1: \quad \theta_y = -k\gamma_t \theta. \tag{10.2}$$

The basic temperature field is piecewise linear and there is no flow.

10.2. Amplitude equations.

Although the notation used in Riahi (1983) is substantially different from that used here, the end result of his analysis is a pair of amplitude equations of the form given by (5.16):

$$A_\tau = R_2 A - A^2 \bar{A} - \Omega(\phi, \gamma_b, \gamma_t) A B \bar{B}, \tag{10.3a}$$

$$B_\tau = R_2 B - B^2 \bar{B} - \Omega(\phi, \gamma_b, \gamma_t) B A \bar{A}, \tag{10.3b}$$

after a certain amount of rescaling of the amplitudes, A and B. A stability analysis of these equations was carried out in §5.3 and it was found that a single roll is stable when $\Omega > 1$ for all relative orientations of the roll and its disturbance. However, whenever $\Omega < 1$, it is possible for three dimensional patterns to be stable, and rolls to be unstable. These three-dimensional patterns tend to be square in planform (i.e. $\phi = 90°$) because the minimum value of Ω is attained by rolls at right angles to one another. Riahi (1983) undertook a detailed survey of variation of Ω as a function of γ_t and γ_b. The following Figure depicts the regions in $\gamma_t - \gamma_b$ space where either rolls or square cells are to be preferred. The classical Darcy-Bénard case corresponds to infinitely large values of γ_t and γ_b, and therefore this confirms the preference for rolls in that case.

10.3. Squares or hexagons?.

Finally we pose a question the answer for which is not yet known. While Riahi (1983) has shown that there are circumstances when squares are to be preferred over rolls, it is quite natural to ask whether it is possible for hexagons to be preferred over squares. In order to begin to answer this question, we'll simply consider the rates of heat transfer for the two different planforms

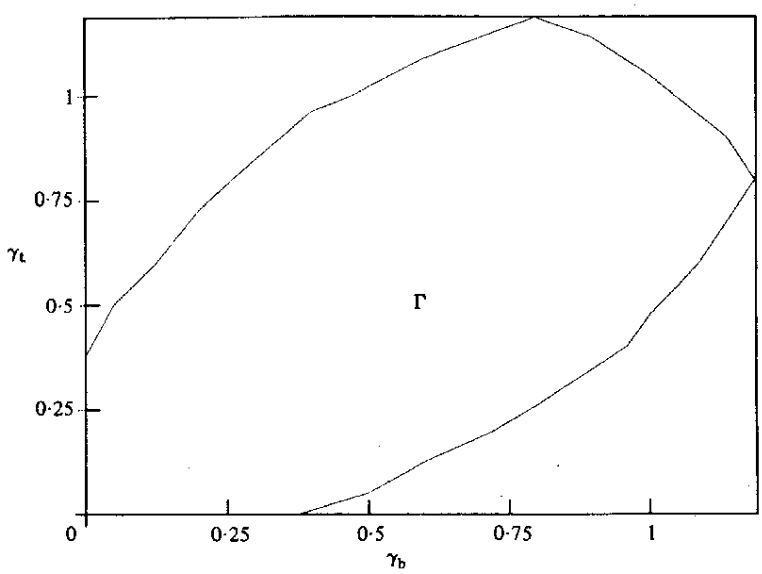

Figure 10.1. Showing Γ, the region of stability for square cell convection, as a function of the conductivities, γ_b and γ_t. Reproduced from Riahi (1983).

(noting that the relative stability of rolls and squares corresponds exactly to which planform has the greater rate of heat transfer — see §5.3.

For squares composed of rolls A and B at mutual orientation $\frac{1}{2}\pi$, the solution is $A = B = \sqrt{R_2/(1+\Omega(\frac{1}{2}\pi)}$ and the rate of heat transfer is

$$\mathrm{HT}_{sq} \propto A^2 + B^2 = \frac{2R_2}{1+\Omega(\frac{1}{2}\pi)}. \tag{10.4}$$

For hexagons composed of rolls A, B and C at mutual orientation $\frac{1}{3}\pi$, the solution is $A = B = C = \sqrt{R_2/(1+2\Omega(\frac{1}{2}\pi)}$ and the rate of heat transfer is

$$\mathrm{HT}_{hex} \propto A^2 + B^2 + C^2 = \frac{3R_2}{1+2\Omega(\frac{1}{3}\pi)}. \tag{10.5}$$

From a heat transfer point of view, hexagons will be preferred to squares when

$$\frac{3R_2}{1+2\Omega(\frac{1}{3}\pi)} > \frac{2R_2}{1+\Omega(\frac{1}{2}\pi)}. \tag{10.6}$$

Hence we must have

$$\Omega(\tfrac{1}{3}\pi) < \tfrac{1}{4}[1+3\Omega(\tfrac{1}{2}\pi)] \tag{10.7}$$

for hexagons to be preferred. At present we do not know if there are any cases in Riahi's problem for which this is so, and therefore it will be necessary to recompute his work.

11. References

H.C.Brinkman (1947) "A calculation of viscous force exerted by a flowing fluid on a dense swarm of particles" *Appl. Sci. Res.* **A1**, 27–34.

X.S. He and J.G. Georgiadis (1990) "Natural convection in porous media: effect of weak dispersion on bifurcation" *J. Fluid Mech.* **216**, 285–298.

J.L.Lage (1998) "The fundamental theory of flow through permeable media from Darcy to turbulence" Transport Phenomena in Porous Media eds. D.B.Ingham & I.Pop. (Springer) 1–30.

D.A.Nield and A.Bejan (1998) "Convection in porous media (2nd Ed.)" Springer.

M. Prats (1966) "The effect of horizontal fluid motion on thermally induced convection currents in porous mediums" *J. Geophys. Res.* **71**, 4835–4848.

D.A.S.Rees (1996) "The effect of inertia on the stability of convection in a porous layer heated from below" *Journal of Theoretical and Applied Fluid Mechanics* **1**, 154–171.

D.A.S.Rees (1997) "The effect of inertia on the onset of mixed convection in a porous layer heated from below" *International Communications in Heat and Mass Transfer* **24**, 277–283.

D.A.S.Rees (2000) "The stability of Darcy–Bénard convection" Handbook of Porous Media ed. K.Vafai. (Begell) 521–558.

D.A.S.Rees (2001) "The onset of Darcy–Brinkman convection in a porous layer: an asymptotic analysis" *Submitted to Int. J. Heat Mass Transfer.*

D.A.S.Rees & D.S.Riley (1986) "Convection in a porous layer with spatially periodic boundary conditions: resonant wavelength excitation" *Journal of Fluid Mechanics* **166**, 503-530.

D.N.Riahi (1983) "Nonlinear convection in a porous layer with finite conducting boundaries" *J. Fluid Mech.* **129**, 153–171.

R.Strange & D.A.S.Rees (1996) "The effect of fluid inertia on the onset of unsteady convection in a saturated porous layer heated from below" *Proc. Int. Conf. on Porous Media and their Applications in Science, Engineering and Industry (June 1996)* Kona, Hawaii, pp71–84.

K.Walker and G.M.Homsy (1977) "A note on convective instabilities in Boussinesq fluids and porous media" *Trans. A.S.M.E. J. Heat Transfer* **99**, 338-339.